FLOW CYTOMETRY IN BIOLOGICAL DOSIMETRY

APOPTOSIS MEASURED BY FLOW CYTOMETRY AS A BIOLOGICAL DOSIMETER – COMPARISON OF ASSAYS AND EFFECTIVENESS OF 280KEV NEUTRONS

By

LORNA RYAN, B.Sc (Hons)

A thesis

Submitted to the School of Graduate Studies

in Partial Fulfilment of the Requirements for the Degree

Master of Science

McMaster University

MASTER OF SCIENCE (2004) (Medical Physics)	McMaster University Hamilton, Ontario

TITLE	Apoptosis Measured By Flow Cytometry as a Biological Dosimeter – Comparison of Assays and Effectiveness of 280kev Neutrons
AUTHOR	Lorna Ryan, B.Sc. (Hons.) (National University of Ireland, Galway)
SUPERVISOR	Dr. Douglas R. Boreham
Number of Pages	xv, 73

ACKNOWLEDGEMENTS

I would like to thank my supervisor Dr. Douglas Boreham for his guidance and support throughout this project. I would also like to express my appreciation to Drs. David Chettle and Jo-Anna Dolling, members of my supervisory committee for their time, assistance and suggestions.

I am very grateful to Jason Fallowdown and Scott McMaster for running the accelerator, and making an endless supply of thick targets for my experiments. I am also grateful to Norbert and Charlie for fixing my computer on numerous occasions.

I am indebted to Melissa Sung, our first co-op student for all her assistance in the lab, her endless patience counting comets and her perpetual cheeriness. I wish to express my sincere thanks to Nicole McFarlane, Mary Ellen Bahen, Jennifer Lemon, Josée Lavoie and Kara Schnarr, my lab family, for all their help, friendship and encouragement. I wish to acknowledge the help received from our collaborators Drs. Ruth Wilkins and James McNamee. I would also like to thank fellow graduate students, who offered support and distraction, especially Anne-Marie MacArtain mo chara mhait as Éirinn.

I wish to thank my friends outside McMaster for reminding me of the world beyond school and making me smile. I would also like to thank Bernadette Rule and Eamonn Ryan for welcoming me to Hamilton many moons ago. Lastly, I would like to express a special thank you to my family, for their eternal optimism, wisdom and endless support from across the miles.

The work described in this study was financially supported by a grant from the Chemical, Biological, Radiological and Nuclear (CBRN) Research and Technology Initiative (CRTI). I am also grateful to McMaster University for the opportunity and financial support offered.

ABSTRACT

It is generally accepted that neutrons are more effective at causing cell damage when compared to X- or gamma radiation. This study, however, indicates that for radiation-induced apoptosis this is not the case. Previously, most RBE (Relative Biological Effectiveness) values for neutrons have been calculated based on chromosome aberrations. In this study the RBE of human lymphocytes after exposure to 280keV neutrons and ^{137}Cs gamma radiation was measured. In the work presented here, the RBE values were calculated based on radiation-induced apoptosis as the biological endpoint and were close to unity. Different markers of apoptosis were compared using flow cytometry assays and microscopy (comet assay). The apoptosis assays measured by flow cytometry were:

- Annexin V conjugated with fluorescein isothiocyanate (FITC) binds to phosphatidylserine exposed on outer leaflet of the cell membrane in apoptotic cells.

- The DNA specific viability dye 7-amino-actinomycin D (7-AAD), binds to the DNA and is excluded from living cells (due to an intact membrane).

- The membrane-permeable lipophilic cationic fluorochrome, 3,3′-dihexyloxacarbocyanine iodide ($DiOC_6$), accumulates in the mitochondria of living cells.

- A DNA intercalating dye propidium iodide (PI), binds to the DNA of dead cells after membrane degradation.

- In addition, FITC conjugated active caspase-3 antibody; caspase-3 is a protein which is activated in apoptotic cells.

Data for a dose response curve were collected for two radiation qualities (280keV neutrons and ^{137}Cs gamma radiation) over a range of acute doses (0, 0.25, 0.5, 1, 2 and 5 Gy). Kinetic studies were done to compare the time course of the apoptosis process by comparing the induction after exposure to either 280keV neutrons and ^{137}Cs gamma radiation at different timepoints over 96 hours. Radiation-induced apoptosis increased with dose, and apoptosis levels peaked between 48 hours and 72 hours depending on the assay which was related to the stage of apoptosis at the time of measurement. For five independent experiments, the two radiation qualities induced similar levels of apoptosis per unit dose.

The purpose of this research was to develop and test different assays to measure apoptosis in human lymphocytes. The specific aim was to compare different radiation qualities and assign an RBE value for low energy fast-neutrons. The overall objective was to determine the sensitivity and feasibility of the different techniques for emergency, accidental, or clinical biological dosimetry. The caspase-3 flow cytometry assay had very good sensitivity at low doses (less than 0.25 Gy). There was a statistically significant difference between the level of apoptosis induced in unirradiated samples and lymphocytes which received 0.25 Gy of neutron or gamma radiation. However, the caspase-3 assay, when compared to other flow cytometry assays, was more time consuming and labour intensive. For speed and simplicity, the

annexin V-FITC and 7-AAD assay was preferable. Both Annexin-V and 7-AAD had good dose response at low doses (0 – 0.25 Gy) but was not as statistically significant as caspase-3 at low doses. Economically, the $DiOC_6$ assay was most feasible; however $DiOC_6$ did not seem very sensitive and had the largest interdonor variation. For sensitivity, simplicity and labour requirements the Annexin V-FITC and 7-AAD assay was the most economical. Overall the comet assay, while technologically being the simplest, was the most labour intensive, as each cell must be scored visually and therefore the most prone to human error.

TABLE OF CONTENTS

LIST OF FIGURES

LIST OF TABLES

LIST OF ABBREVIATIONS

7 – AAD	7-Amino-Actinomycin D
AIF	Apoptosis Inducing Factor
Apaf-1	Apoptotic Protease Activating Factor
BSA	Bovine Serum Albumin
Caspases	Cysteinyl Apartate-Specific ProteinASES
CD95	Cluster Designation 95
DIABLO	Direct IAP Binding protein with low pI
$DiOC_6$	3,3′-Dihexyloxacarbocyanine Iodide
DNA	Deoxyribonucleic Acid
EDTA	Ethylenediamine Tetraacetate
FADD	Fas-Associated protein with Death Domain
FITC	Fluorescein Isothiocyanate
FLIP	FLICE-like inhibitory protein
LET	Linear Energy Transfer
PBS	Phosphate-Buffered Saline
PI	Propidium Iodide

PMT	Photomultiplier Tube
PS	Phosphatidylserine
RBE	Relative Biological Effectiveness
RPMI	Roswell Park Memorial Institute
SMAC	Second Mitochondrial-derived Activator of Caspase
TAE	Tris Acetate EDTA Buffer
TMP	Transition of the Mitochondrial Transmembrane Potential

1 INTRODUCTION

1.1 Apoptosis and Radiation

In recent years, concern about the biological effects of neutrons has grown due to occupational exposures from increased high-altitude travel, longer space missions and the production of neutrons in nuclear power plants. In addition, international acts of terrorism could potentially expose humans and biota to neutrons. In general, people may be exposed to wide range of neutron energies, from low thermal energies (a few eV) to high MeV energies.

One of the major challenges facing biological dosimetry is the ability to measure accurately the biological damage and the subsequent risks associated with radiation exposure. It has previously been reported that programmed cell death or apoptosis, of white blood cells may be a useful biological indicator of radiation exposure (Menz *et a.*, 1997; Boreham *et al*, 1996) as apoptosis is a form of cell death that has distinctive morphological and biochemical characteristics (Steller, 1995). Apoptosis (interphase cell death or programmed cell death) is the primary mode of radiation-induced cell killing in human lymphocytes. Other forms of cell death include necrosis, mitotic catastrophe and clongenic death; all are very distinctive compared to apoptosis.

Apoptosis is morphologically characterized by increased cytoplasmic granularity, cell shrinkage, chromatin condensation, membrane blebbing and loss of plasma membrane asymmetry (Kerr *et al*, 1972; Wyllie, 1995; Willingham, 1999;

Strasser *et al*, 2000). A cartoon diagram of the morphological changes which a cell undergoes, as it becomes apoptotic is shown in Figure 1-1 (Saini and Walker, 1998). Ionizing radiation is a DNA damaging agent which induces apoptosis in some cell types, including human lymphocytes. Biochemically, cells undergoing apoptosis are characterized by depolarization of the mitochondrial membrane electrochemical gradient, loss of plasma membrane symmetry which results in externalization of phosphatidylserine residues on outer surface of plasma membrane, and finally DNA cleavage followed by rupture of the plasma membrane (Schultz and Harrington, 2003; Kroemer and Reed, 2000; Budihardjo *et al* 1999; Cryns and Yuan, 1998). (See Figure 1-1)

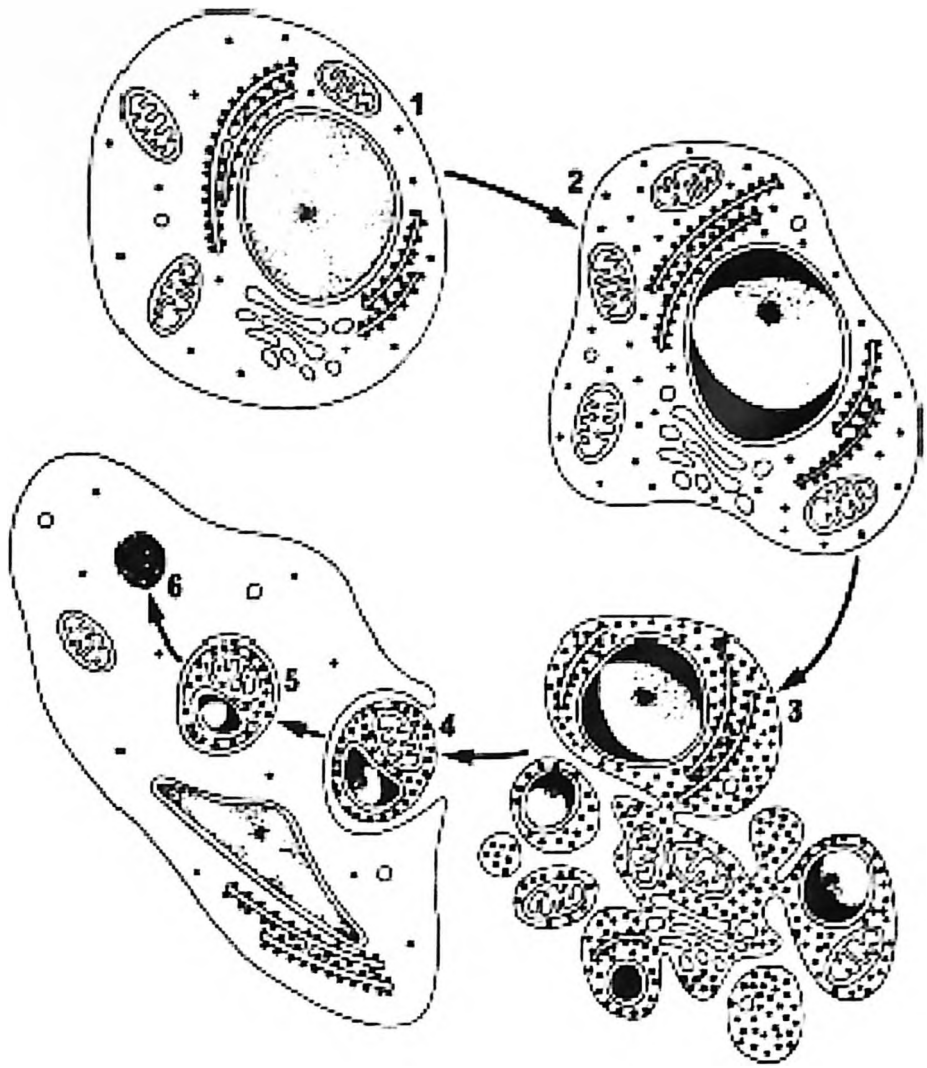

Figure 1-1. The morphological changes associated with apoptosis. A morphologically normal cell (1). Segregation of chromatin in sharply circumscribed masses (2). Nucleolar changes also occur (2 and 3). Fragmentation of the nucleus and blebbing of the cell as a whole occurs which produces membrane-bound apoptotic bodies of various sizes and shapes (3). These apoptotic bodies are phagocytosed by neighbouring cells (4), are degraded within the lysosomes (5) and finally reduced to residuals (6). (Taken from Saini and Walker, 1998).

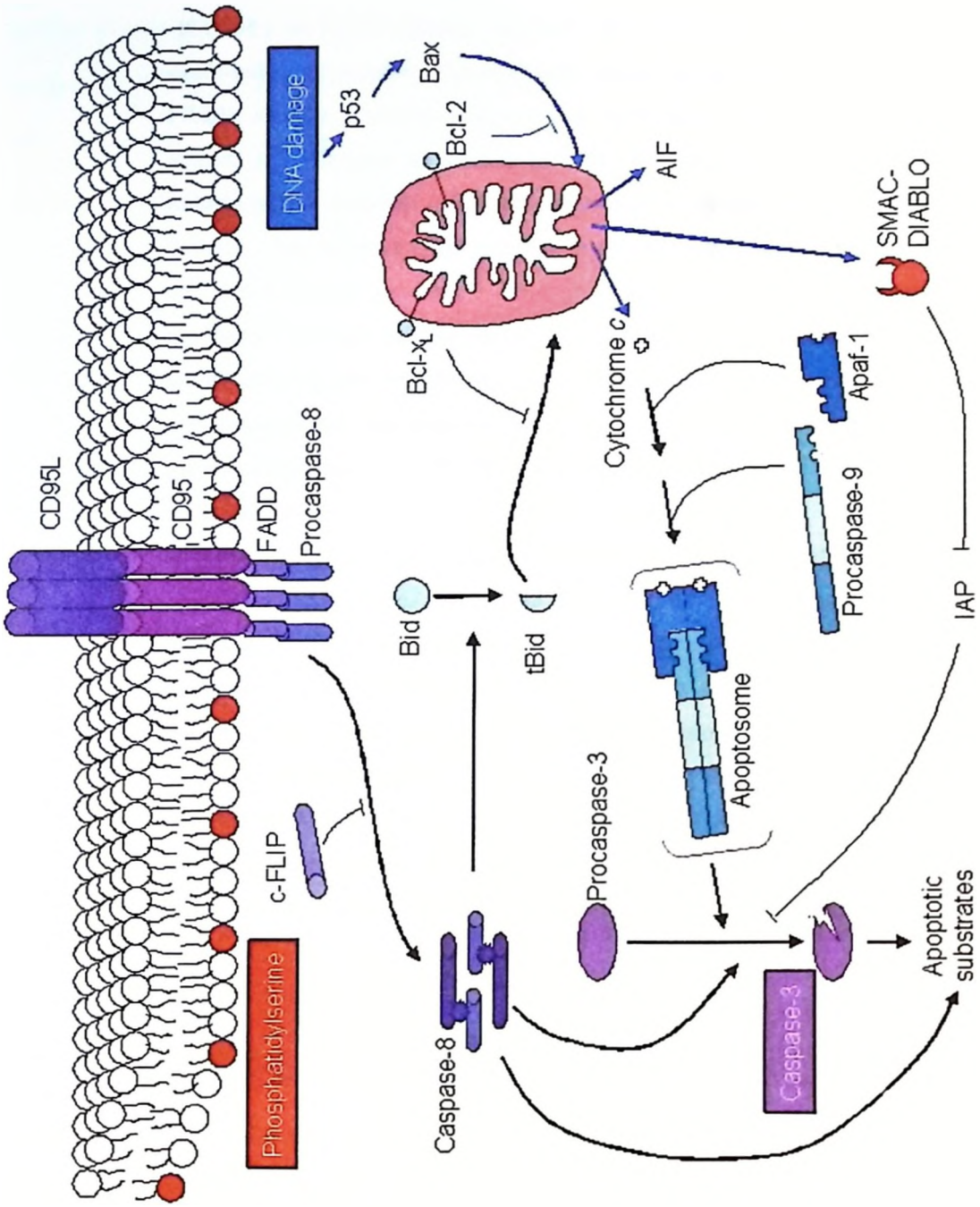

Figure 1-2. The death receptor pathway (purple), is triggered by members of the death-receptor superfamily (CD95). The binding of CD95 ligand

(CD95L) to CD95 induces receptor clustering and formation of a death-inducing complex, Fas-associated death domain protein (FADD). FADD recruits multiple procaspase-8 molecules, causing caspase-8 activation. Caspase activation may be blocked by c-FLIP. The mitochondrial pathway (blue) is a response to insults such as DNA damage. The mitochondrial pathway is regulated through activation of the Bcl-2 family proteins. Pro- and anti-apoptotic Bcl-2 family members converge on the surface of the mitochondria, where they compete to regulate cytochrome *c* release from the mitochondria. If the pro-apoptotic proteins dominate, an array of molecules is released from the mitochondrial compartment, including cytochrome *c*. Cytochrome *c* associates with Apaf-1 and then procaspase-9 to form the apoptosome. The death receptor and mitochondrial pathways converge at caspase-3 activation. Caspase-3 activation may be antagonized by inhibitor of apoptosis proteins (IAP); however IAPs themselves are disrupted by SMAC/DIABLO protein which is released by the mitochondria. After Caspase-3, the apoptotic program branches into multiple sub-programmes, resulting in the ordered dismantling and removal of the cell from the population of lymphocytes. Early apoptosis is marked by loss of membrane asymmetry which results in the exposure of phosphatidylserine on the outer leaflet (red, Figure 1-3).

Several methods have been developed to detect apoptosis in cells as a result of exposure to ionizing radiation. Generally methods are based on either morphological or biochemical changes. These assays which provide quantitative information on apoptosis include; DNA laddering (Overbeeke *et al* 1998), *in situ* nick translation (Loo and Rillema, 1998; Sgonc and Grubber, 1998), terminal deoxynucleotydyl transferase mediated dUTP nick end labelling (TUNEL) (Sgonc *et al*, 1994), terminal

deoxynucleotydyl transferase (TdT) assay (Gorczyca *et al*, 1993) and fluorescence analysis of DNA unwinding (FADU) (Cregan *et al*, 1994). Most of these methods are time consuming and labour intensive, consequently improved techniques have been developed. Due to high throughput capability, flow cytometry has become a rapid and a useful method for detecting apoptosis. As flow cytometry is able to analyze several parameters simultaneously it is capable of detecting both morphological and biochemical changes in cells. For example, it can detect a change in cell size and granularity while measuring the binding of fluorescently conjugated antibodies or fluorescent stains which are targeted to DNA or proteins unique to apoptotic cells. Flow cytometry has the ability to provide a fast, efficient and cost effective method of measuring apoptosis and therefore useful in determining the magnitude of the biological effect or the relative risk associated with radiation exposure.

A variety of flow cytometry assays which allow sensitive and rapid detection of apoptotic cells have been reported. During early stages of apoptosis there is the formation of mitochondria megachannels (permeability transition pores) in the outer membrane leaflet. When these megachannels open, the asymmetric distribution of protons on both sides of the inner mitochondrial membrane is lost. This is known as transition of the mitochondrial transmembrane potential (TMP) (Vermes *et al*, 2000; Martinou, 1999). In living cells the inner side of the inner mitochondrial membrane is negatively charged; this allows cationic lipophilic fluorochromes to accumulate in the mitochondria. Therefore, an early sign of apoptosis is the inability of a cell to accumulate a lipophilic fluorochrome such as dihexyloxacarbocyanine iodide ($DiOC_6$). By combining $DiOC_6$ with a DNA intercalating dye, such as propidium iodide (PI), apoptotic and necrotic cells can be distinguished (Vermes *et al.*, 2000).

The differentiation is possible, as $DiOC_6$ will accumulate in living cells while an intact membrane will exclude PI, PI will only be detectable in dead cells which have lost their membrane permeability.

An early indicator of apoptosis is the expression of phosphatidylserine (PS) on the outer leaflet of the plasma membrane (externalization) (Fadok *et al.*, 1992; Castedo *et al*, 1996). It has been suggested that the PS externalization may occur after early caspase activation and may happen during the early-execution phase (Van Engeland *et al*, 1998). The translocation of PS to the outer membrane surface can be detected by annexin V. Annexin V is a protein which binds in a calcium dependent manner to the exposed PS (Figure 1-3). Using annexin V conjugated with fluorescein isothiocyanate (FITC), in combination with the DNA specific viability dye 7-amino-actinomycin D (7-AAD) (which is excluded from living cells and therefore those cells are non fluorescent), early and late stages of apoptosis can be determined (Wilkins *et al.*, 2002; Rasola and Geuna, 2001; Hertveldt *et al.*, 1997). Recently the kinetics of PS expression has been questioned and it has been suggested that PS exposure may occur after early caspase activation and is possibly an early phenomenon of the execution phase (Van Engeland *et al*, 1998). However if one is not concerned about the exact kinetics of PS exposure, this current debate does not affect the validity of using annexin V-FITC as a measure of apoptosis.

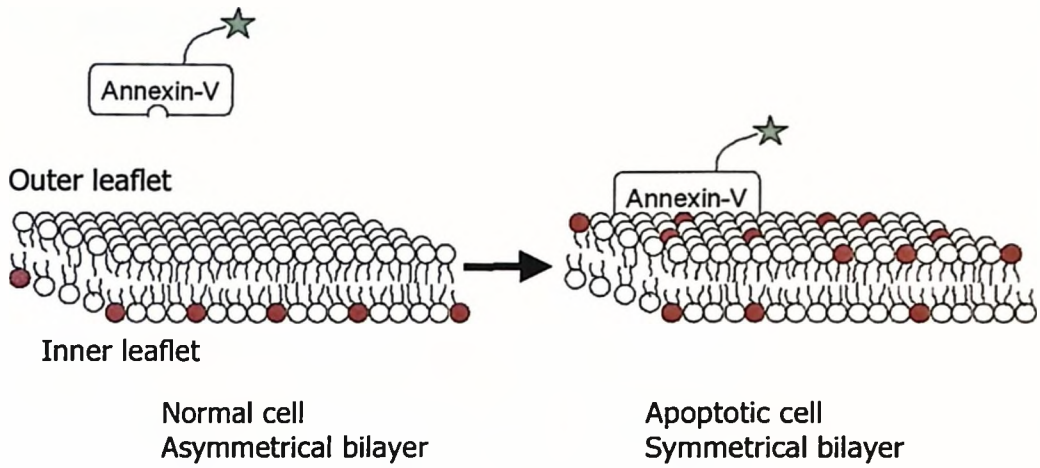

Figure 1-3. Schematic representation of the loss of membrane asymmetry during apoptosis. Live cells have an asymmetric membrane, the phosphatidylserine residue (red dots) remains on the inner leaflet of the lipid bilayer. During apoptosis the PS residues become exposed to the outer membrane leaflet. Annexin V binds with high affinity to the exposed PS in the presence of Ca^{+}.

Active Caspase-3 is another marker for cells undergoing apoptosis. Caspase-3 is a key effector in the apoptosis pathway. It amplifies the signal from initiator caspases (such as caspase-2 and caspase-8) signifying full commitment to cellular disassembly. Using an antibody conjugated with FITC and specific to the active form of caspase-3 antibody, it is possible to quantify the levels of caspase-3 in a cell as it undergoes apoptosis (Gown and Willingham, 2002; Budihardjo *et al*, 1999; Belka *et al*, 1999; Cryns and Yuan, 1998)

1.1.1 Relative Biological Effectiveness

It has been reported that neutrons are more efficient per unit dose compared to X- or gamma-radiation at causing cell damage in human lymphocytes (Schmid *et al*, 2003, 2002, and 2000; Prasanna *et al*, 1997; Fabry *et al*, 1985; Bauchinger *et al*, 1984). In those studies the radiation-induced cell damage was assessed using cytogenetic analysis. This increased efficiency is known as the relative biological effectiveness (RBE), and is defined as the ratio of the dose from some standard photon beam (usually 250keV X-rays) divided by the dose of the test exposure that is necessary to produce the same level of biological effect (Figure 1-4).

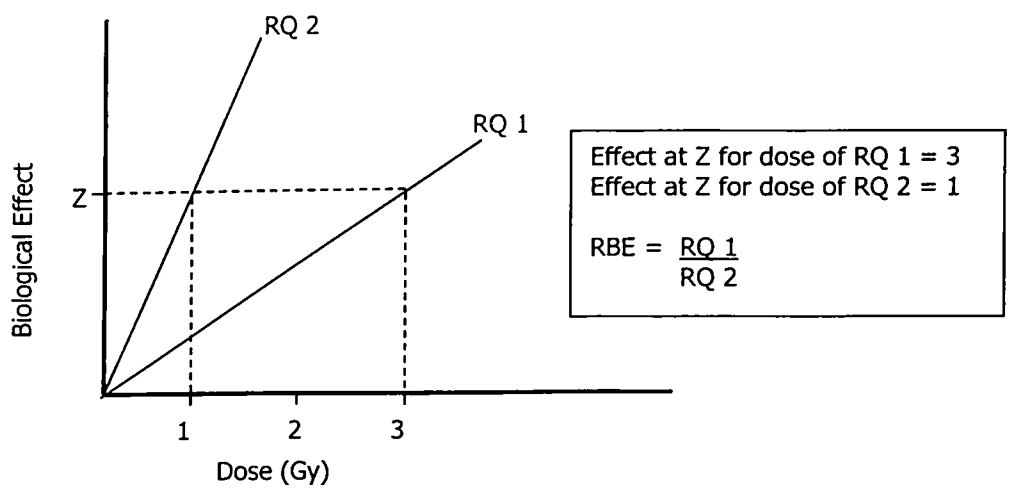

Figure 1-4. Calculation of relative biological effectiveness (RBE). RQ 1 is the dose response curve for reference radiation (usually 250 keV X-rays). RQ 2 is the dose response curve for the test radiation quality. Z is the point where the biological effect of the two radiation qualities is the same. In this example the dose of RQ 2 is three times lower than the dose of RQ 1 for the same effect. Therefore the RBE for radiation quality equals three.

1.1.1 Relative Biological Effectiveness

It has been reported that neutrons are more efficient per unit dose compared to X- or gamma-radiation at causing cell damage in human lymphocytes (Schmid *et al*, 2003, 2002, and 2000; Prasanna *et al*, 1997; Fabry *et al*, 1985; Bauchinger *et al*, 1984). In those studies the radiation-induced cell damage was assessed using cytogenetic analysis. This increased efficiency is known as the relative biological effectiveness (RBE), and is defined as the ratio of the dose from some standard photon beam (usually 250keV X-rays) divided by the dose of the test exposure that is necessary to produce the same level of biological effect (Figure 1-4).

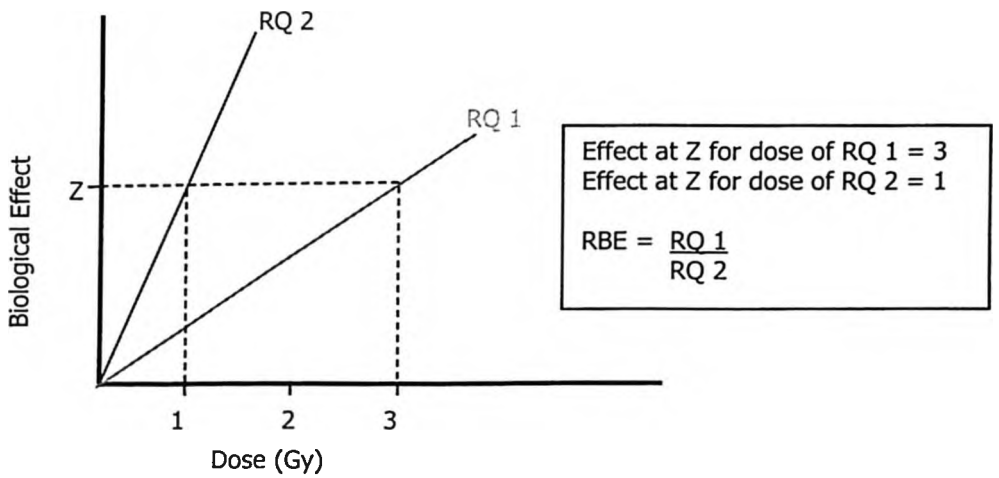

Figure 1-4. Calculation of relative biological effectiveness (RBE). RQ 1 is the dose response curve for reference radiation (usually 250 keV X-rays). RQ 2 is the dose response curve for the test radiation quality. Z is the point where the biological effect of the two radiation qualities is the same. In this example the dose of RQ 2 is three times lower than the dose of RQ 1 for the same effect. Therefore the RBE for radiation quality equals three.

The enhanced effectiveness of neutrons is thought to be a result of the increasing ionization density of its recoil products, compared to the fast electrons induced by X- and gamma- radiation. In this study the ability of 280keV neutrons to induce apoptosis in human lymphocytes was compared to ^{137}Cs gamma radiation. Due to the high density of ionization tracks made by high-linear energy transfer (LET) radiation such as neutrons, clustered damage is produced when these tracks hit primary molecular targets (Goodhead, 1994). There have been inconsistent results published describing the RBE of fast neutrons for cell killing. Warenius and Down (1995) reported an RBE of one for the induction of apoptosis by 62.5 MeV fast neutrons in mouse thymocytes. Vral *et al.* (1998) reported an RBE of unity for the induction of apoptosis by 14.5MeV neutrons in human lymphocytes. Hendry *et al.* (1995) reported RBE values for 14 to 600 MeV neutrons between 3 and 4 in intestinal crypt cells and Meijer *et al* (1998) has reported an RBE of 1.3 to 3.0 for apoptosis in human lymphocytes when comparing ^{137}Cs to 32-45MeV nitrogen ions (Table 1-1 for summary). The variability of results, the different biological endpoints and the varying neutron energies support the need for further studies if apoptosis is going to be used in biological dosimetry. This study reports on the level of apoptosis induced in human peripheral lymphocytes, using two radiation qualities and different assays that can detect various stages of the apoptotic process.

Table 1-1. A Summary of recently published high LET RBE studies.

Radiation Quality	End Point	Cell Type	RBE	Author	Year
62.5MeV neutrons	apoptosis	mouse thymocytes	62.5	Warenius & Down	1995
14.5MeV neutrons	apoptosis	human lymphocytes	1	Vral *et al*	1998
14 - 600MeV neutrons	apoptosis	intestinal crypt cells	3 - 4	Hendry *et al*	1995
32 - 45MeV nitrogen ions	apoptosis	human lymphocytes	1.3 - 3.0	Meijer *et al*	1998
65keV neutrons	chromosome aberrations	human lymphocytes	2.4	Prasanna *et al*	1997
36.6 - 14.6keV neutrons	dicentrics	human lymphocytes	16.6 - 23.4	Schmid *et al*	2003

1.2 Flow Cytometry

In flow cytometric analyses, a single cell is individually interrogated as it passes through a focused beam of light. The single-file stream of cells is created by delivering the sample through a small-bore injection needle into a larger stream of rapidly flowing sheath fluid. The creation of a narrow, central focused sample core stream within the sheath stream is accomplished by the acceleration of the sample stream as it enters the sheath stream. The core sample stream has a diameter of the order of a cell diameter or slightly larger. The width of the sample stream may be varied by adjusting the sample delivery velocity relative to the sheath velocity (Figure 1-5).

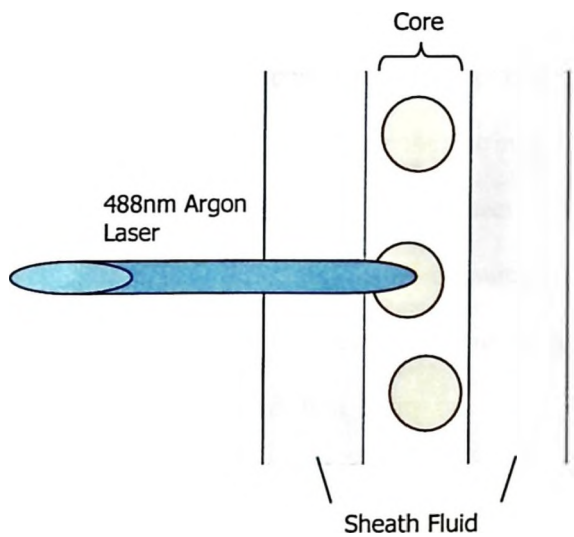

Figure 1-5. The cell interrogation point of a flow cytometer. Cells pass the elliptically focused 488nm laser beam in a single file. Hydrodynamic focusing is used to confine the cell containing core fluid in a narrow stream within a flowing stream of cell free sheath fluid. The two streams travel at different velocities, thus remaining separate. Using

conservation of mass, the same volume of the narrower stream must pass the interrogation point in the same time interval. Therefore the core stream must be at a faster velocity. By adjusting the speed of the core stream one can adjust the volume of sample and number of cells analysed per unit time analysed.

The light source consists of a 488nm air-cooled argon laser, and the beam is focused into a 10μm × 80μm ellipse by a pair of crossed cylindrical lenses aligned perpendicular to each other. The laser is focused such that the long axis of the ellipse is perpendicular to the flow of the sample stream. An ellipse is used in this fashion to minimize fluctuations in the intensity of interrogating light to the passing cell. Cells interact with the focused laser beam to give either intrinsic or extrinsic measurements. The cell interacts with the focused beam of light by scattering in either the forward (180°) or side (90°) angles, which are the intrinsic measurements of cell size and granularity. It is also possible for the light to react with dye molecules associated with specific cellular constituents (extrinsic measurements). Extrinsic measurements usually assess the intensity of fluorescence emitted by fluorescent molecules which were added to the cells and that stain or are associated with specific cellular constituents such as DNA (Figure 1-6).

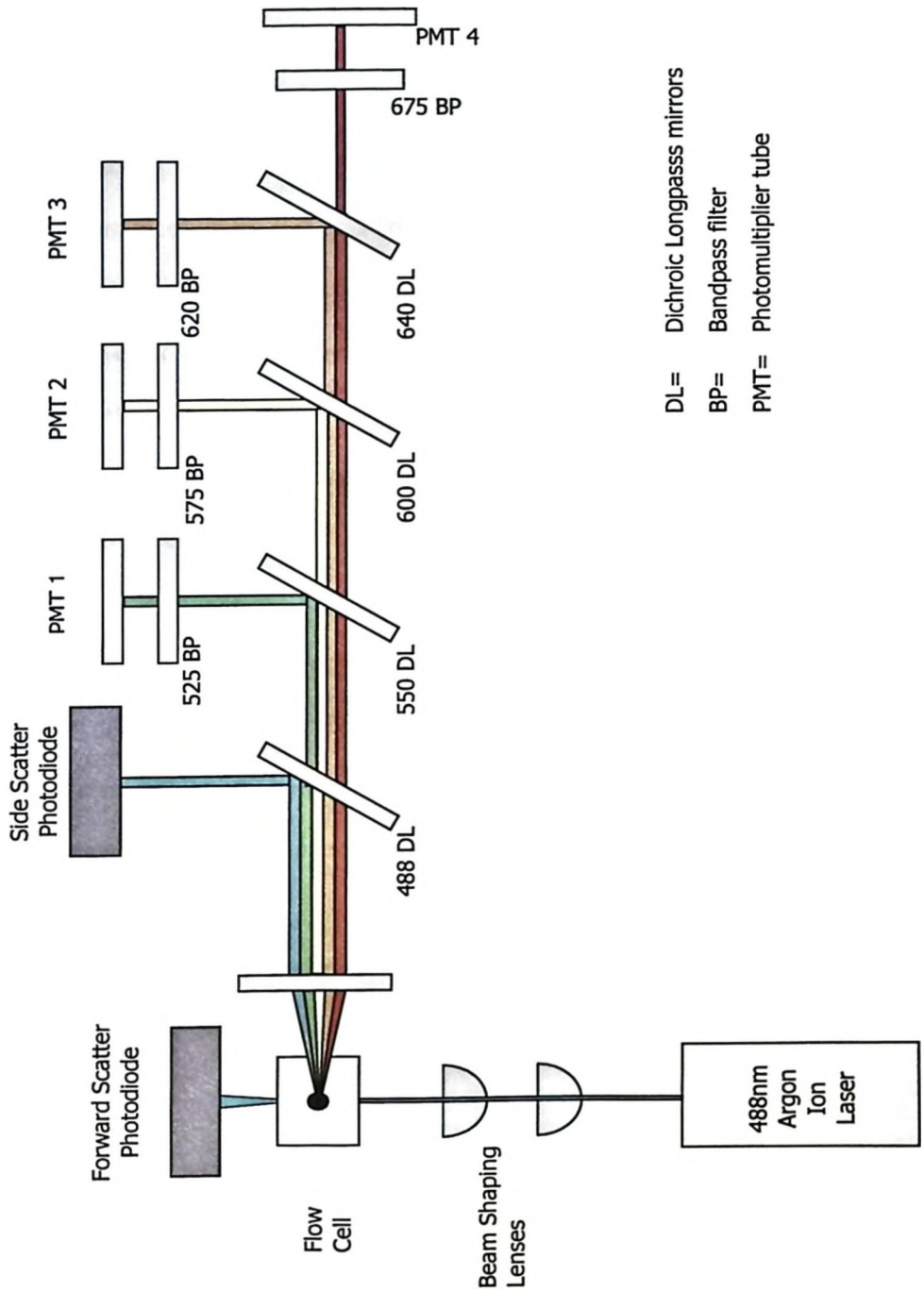

Figure 1-6. Schematic of the laser, bandpass filters and detectors used in a flow cytometer.

The scattered light is measured by a number of light-sensitive detectors. The detectors used are either photodiodes or photomultiplier tubes (PMTs). A photodiode is a silicon solid-state device in which impinging photons excite electrons from a nonconducting band in a proportional manner resulting in an output current. The current produced is proportional to the number of incident photons. In PMTs, the incident photon impinges on the photocathode and excites or releases an electron into a vacuum enclosure. The electrons are accelerated by a potential difference through a series of electrodes (a dynode chain, each dynode has a slightly more positive charge than its neighbour dynode nearer the photocathode); at each stage of the chain the collision of electrons with the surface of the electrodes causes the release of additional electrons (Figure 1-7). Thus, in a PMT, there is an exponential increase in the number of electrons released at the end of the dynode chain, which is proportional to the initial number of photons that initially impinged on the photocathode. The current emitted per incident photon can be increased by increasing the potential difference across the PMT, thus it is possible to increase the sensitivity of the PMTs.

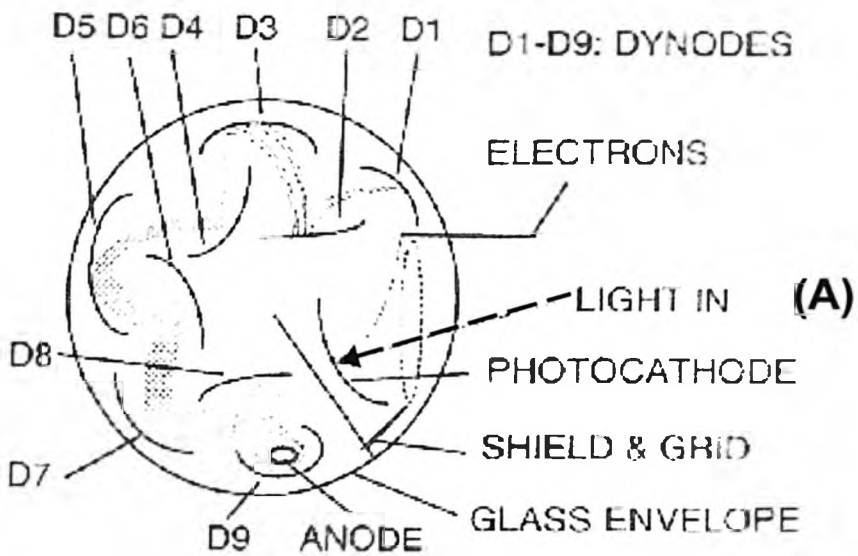

Figure 1-7. Elements of a Photomultiplier tube (PMT). A single photon enters and intersects with the photocathode causing the release of electrons (A). The electrons are attracted to the first dynode (D1), where they impinge on the surface causing the release of additional electrons. The additional electrons are accelerated to the second dynode (D2) by an increasing potential difference where the process is repeated. Additional electrons are produced in an exponential fashion in dynodes along the chain. The multiplication of electrons results in a signal which is detectable by the anode. PMTs are required for detecting the emitted fluorescence, as the intensities of the signal are weak (Shapiro HM, 2003, p 160).

Photons from the incident laser beam are scattered as a single cell passes through the focal point and these photons are collected by the photo-detectors. Two different geometries are examined, the first is a few degrees from the axis of the incident laser beam (forward scatter), the second photo-detector is at 90° to the

incident laser beam (side scatter). It is generally accepted that forward scatter correlates with cell size. This allows the discrimination of debris and aggregates, as well as identifying cells of differing sizes. Side scatter light intensity is significantly affected by cellular structure and complexity (for example, the intensity of side scatter increases with increasing granularity), however the side scatter is also dependent on cell-size. These interactions are related to cellular characteristics in a complex way. Therefore side scatter can only give approximate information about the cellular structure. The combination of forward and side scatter light measurements allows the differentiation of peripheral blood leukocytes, into lymphocytes, monocytes and granulocytes. Most of the information required for discriminating leukocytes is obtained from the side scatter signal, which is low for lymphocytes, higher for monocytes and highest for granulocytes. The granular structure of granulocytes produces many more opportunities for the scattering of incident light than the scattering from the more uniform cytoplasm and nucleus of lymphocytes (Figure 1-8).

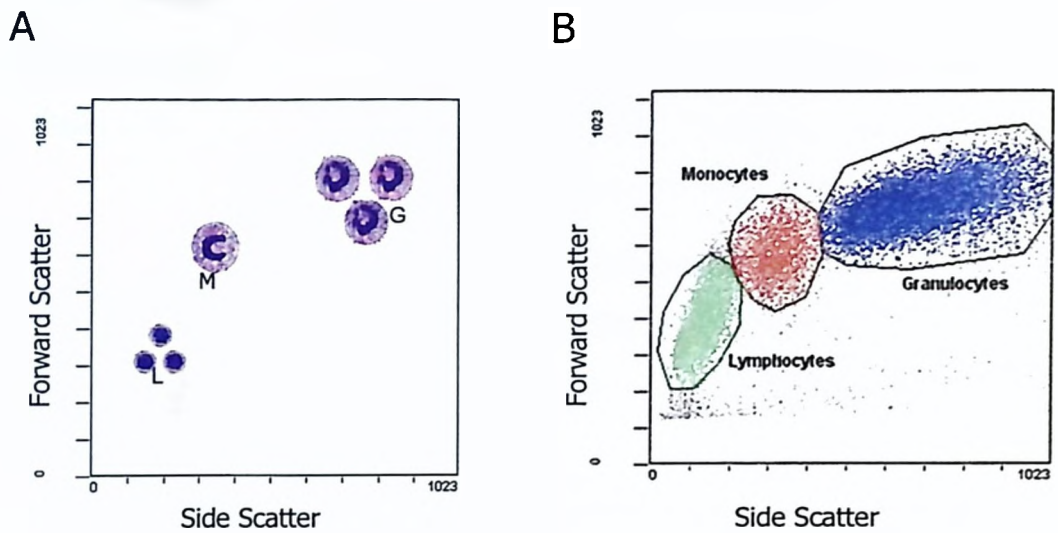

Figure 1-8. (A) Cartoon representation of leukocytes, showing uniform cytoplasm of lymphocytes (L) and increasing granularity and size of monocytes (M) and granulocytes (G). (B) Data collected from Beckman Coulter Epics XL flow cytometer showing leukocyte gating strategy.

As the intensity of fluorescent emissions is much less than that of scattered light, PMTs are used in detection of fluorescence. Though fluorescent light is emitted in an isotropic distribution, it is only measured at 90° to the incident laser beam. However, while it is possible to use multiple fluorescent probes simultaneously, it is necessary to separate the different fluorescent emission wavelengths using interference filters, also called dichroic filters. The filters used are band pass and long pass filters. The long pass dichroic mirrors reflect shorter wavelength light through a 90° angle, towards the photo-detector. The dichroic long pass filters used in the EPICS® XL are, 488, 550, 600 and 645nm. Bandpass filters specific for the wavelength (fluorescent colour) of interest are then used to purify further the light

entering the detector. For the EPICS® XL flow cytometer the bandpass filters used are 525, 575, 620 and 675nm for green, yellow, orange and red respectively (Figure 1-6 and Figure 1-15)

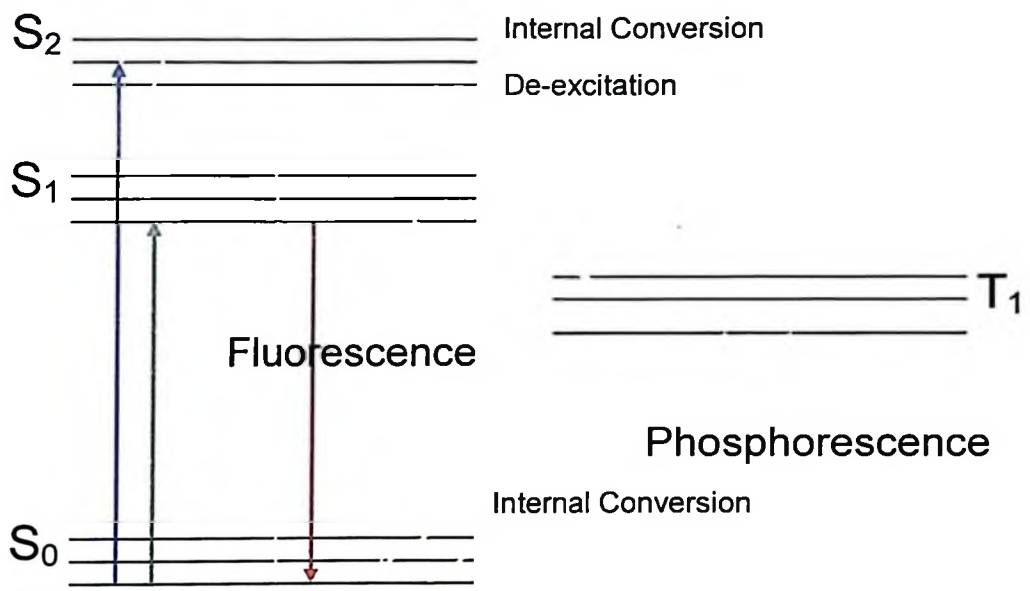

Figure 1-9. The Jablonski diagram of electronic energy levels and transitions. Solid straight arrows show radiative transitions and wavy arrows show nonradiative transitions.

Fluorescence occurs due to the excitation and subsequent relaxation of molecules. In Figure 1-9, an electron resting in ground state, S_0, absorbs energy. Immediately following absorption, the molecules involved are likely to be in a higher vibrational excited state associated with S_1 or S_2. If the molecule has been excited to S_2 it loses the excess electronic energy by internal conversion and vibrational relaxation, which are nonradiative transitions. That is, an electronic change in energy

state which is not accompanied by emission of photons. When the excited electrons reach the lowest vibrational energy level of S_1 they can relax back to the ground state by either fluorescence or phosphorescence. Fluorescence occurs when electrons in the S_1 excited state return to the ground state by emission of photons. Since the excited electron loses some of its energy through internal conversion, and vibrational relaxation following fluorescence, the photons emitted by fluorescence will be at a lower energy and longer wavelength than the absorption which preceded it.

The wavelength difference which occurs between the excitation maximum and the emission maximum is known as Stokes shift. Figure 1-10 shows the excitation and emission spectrum for fluorescein, the fluorescent constituent of FITC, a commonly used fluorescent probe.

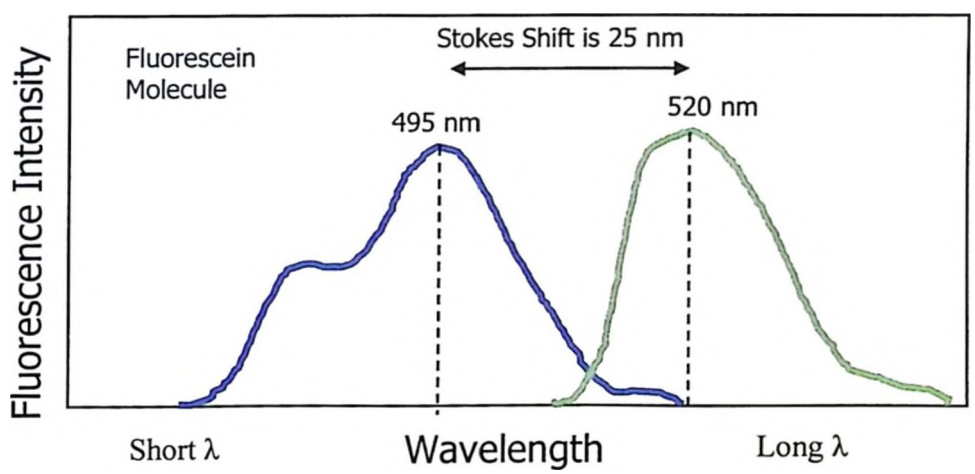

Figure 1-10. Stokes Shift is the energy difference between the lowest energy peak of absorbance and the highest peak energy of emission

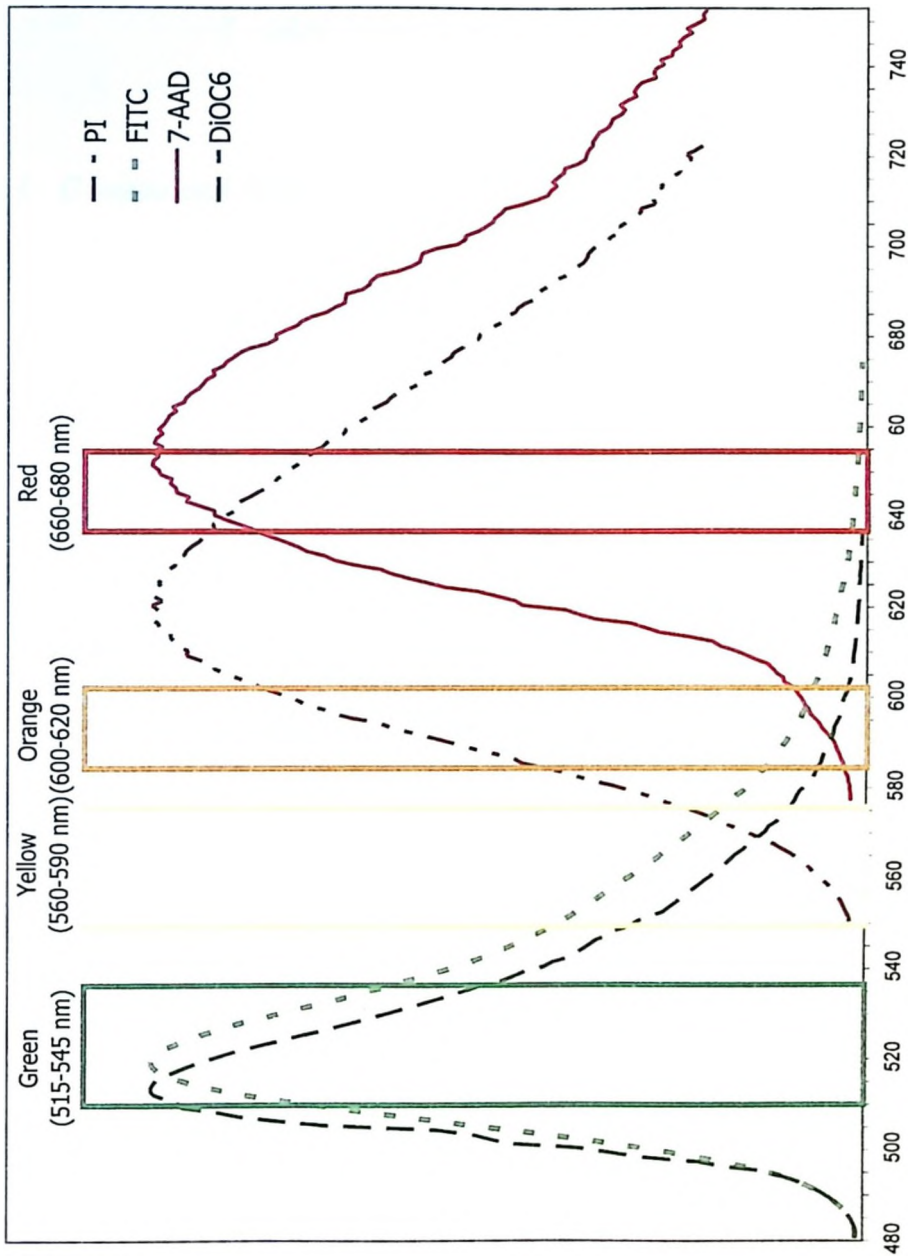

Figure 1-15. The emission spectra shown are for fluorescein isothiocyanate (FITC), dihexyloxacarbocyanine iodide ($DiOC_6$), propidium iodide (PI) and 7- aminoactinomycin D (7-AAD). Boxes indicate the passbands of green (525nm), yellow (575nm), orange (620nm) and red (675nm) filters.

2 MATERIALS AND METHODS

2.1 Gamma and Neutron Irradiation

2.1.1 Human Lymphocyte Collection

Venous blood samples (24 ml per volunteer) were collected from six healthy volunteers, (four male and two female) in heparinized Vacutainer tubes (Becton Dickinson, Franklin Lakes, NJ) and were held at ambient room temperature in an insulated container until irradiation. Whole blood was irradiated (in Vacutainer tubes) at room temperature with either ^{137}Cs or 280keV neutrons at a constant dose rate of approximately 2 Gy h^{-1}. The time between blood collection and start of irradiation did not exceed 20 minutes.

2.1.2 Neutron Irradiation

Continuous energy spectra of neutrons with a mean energy of 280keV (hereafter the neutron beam is described as 280keV neutrons, though the energy ranges up to 520keV) were produced by means of the $^{7}Li(p,n)^{7}Be$ reaction. Samples were irradiated at a source to target distance of 5cm and at an angle of zero degrees with respect to the direction of the ion beam. To maintain a steady dose rate while exposing the samples, the beam was constantly monitored during all experiments using an Anderson and Braun rem counter and BF_3 detectors, which were located at

different fixed positions inside the irradiation room. The dose rate was held constant throughout all experiments by adjusting the proton beam current on the Li target. Dose rate was measured by an established technique which uses a tissue equivalent proportional counter (TEPC) (Aslam *et al.* 2003a, 2003b, 2003c, and 2003d Khan, 2003, Arnold, 2001). The uncertainty of dose measurement was less than 15% at the 95% confidence interval.

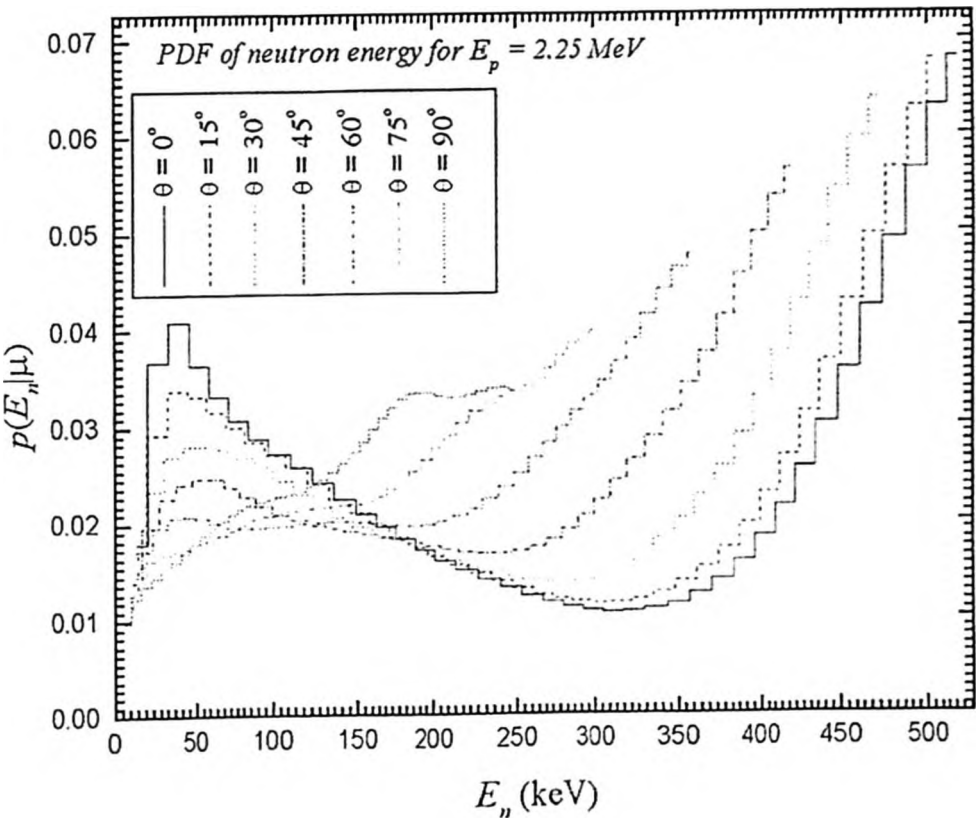

Figure 2-1. Energy distribution of neutrons produced from a proton beam energy E_p= 2.25 MeV on a thick lithium target causing the (p,n) reaction emitting neutrons with a mean energy of 280keV (Taken from Aslam, 2003d).

2.1.3 ^{137}Cs Gamma Irradiation

Exposure to gamma radiation was by ^{137}Cs gamma cell with an exposure rate of 0.35 Roentgen per minute, which corresponded to a dose rate of $2.06Gyh^{-1}$ in water. Samples were irradiated at a source to sample distance of 92cm in the centre of the collimated beam. The dosimetry was performed by using a pre-calibrated Farmer dosimeter with a $0.6\ cm^3$ chamber. The chamber calibration could be traced to the primary standard laboratory at the National Research Council of Canada (Figure 2-2). The uncertainty of dose measurement was less than 5% at the 95% confidence level.

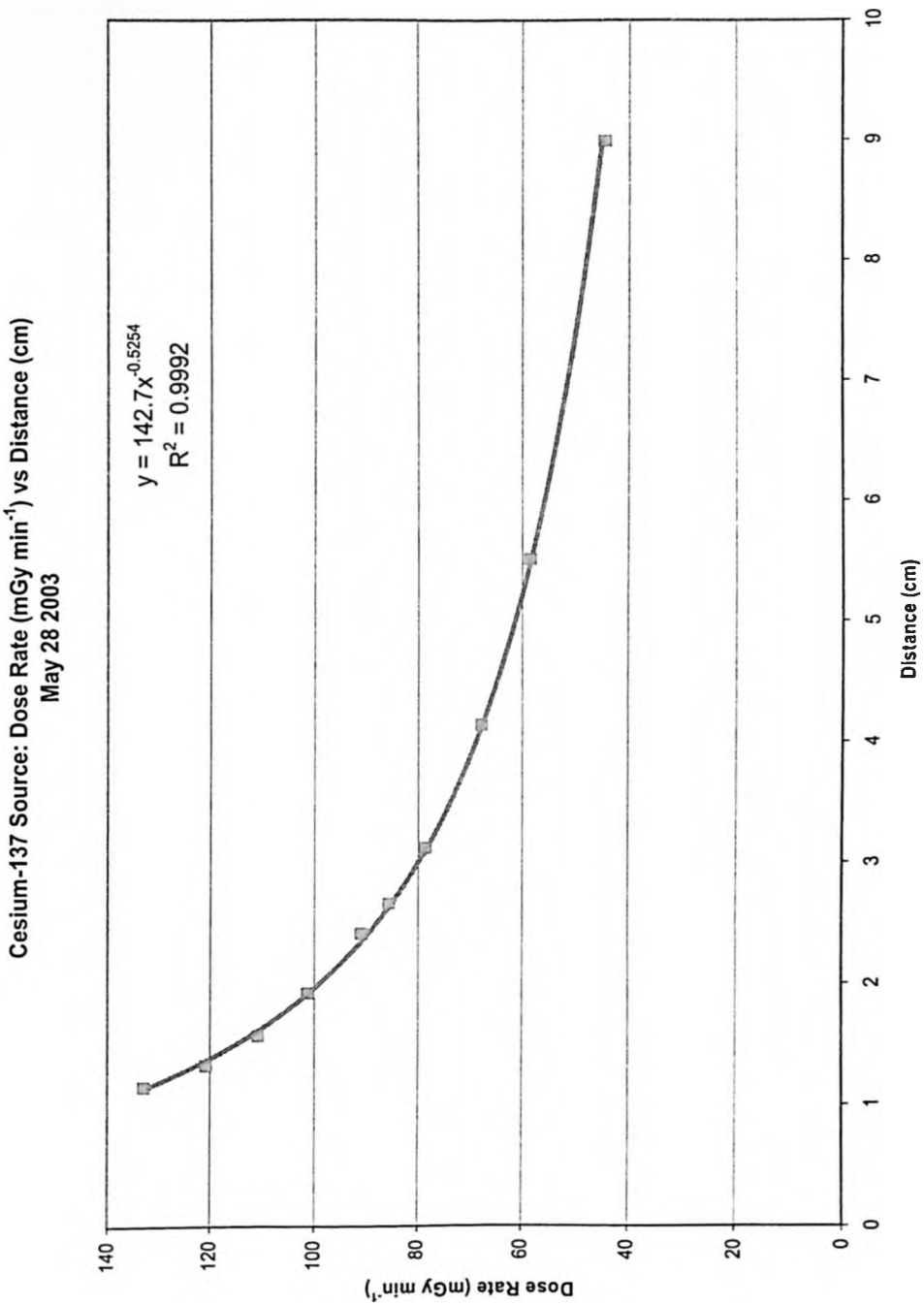

Figure 2-2. Dose rate map for, Taylor Radiobiology Facility ^{137}Cs source at McMaster University

2.2 Cell Culture

Immediately following irradiation, mononuclear lymphocytes were isolated from whole blood as follows. Whole blood was mixed 1:1 with 1 x phosphate-buffered saline (PBS) (137 mM NaCl, 2.7 mM KCl, 4.3 mM Na_2HPO_4 and 1.4 mM K_2PO_4). Blood and PBS mixture (7ml total) was then layered over 3ml of Histopaque-1077 (Sigma Diagnostics, St. Louis, MO) in a 15ml centrifuge tube and separated by density centrifugation (200g for 30 minutes at room temperature). The isolated lymphocyte layer was removed from Histopaque and washed once in 7ml of 0°C PBS, then in 7ml of 0°C complete RPMI-1640 medium, (RPMI 1640 media supplemented with, 20% Fetal Bovine Serum, 2mM L-glutamine, 10 U ml^{-1} and 10 μG ml^{-1} streptomycin sulphate). Cell number was determined using a Beckman Coulter Z2 Coulter Particle Counter and Size Analyzer. The protocol followed was suggested by the manufacturer; 20 μl of sample was placed in 10 ml of Isoflow™ Sheath fluid (Beckman Coulter, Fullerton, CA), 3 drops of Zap-oglobin™ II lysis solution (Beckman Coulter, Fullerton, CA) were added, the sample was capped and inverted. After two minutes incubation at room temperature the sample was run on the Z2 counter, lymphocytes were identified as having a particle size greater than 17.5 μm. The cells were then diluted to 4.0 x 10^5 cells ml^{-1} in the complete RPMI 1640 medium at 37°C. A minimum of 5ml of cell culture was incubated in T-25 culture flasks (Nalge Nunc International, Rochester, NY) at 37°C, 5% CO_2 and 98% relative humidity.

2.3 Apoptosis Measurements

Three flow cytometry assays (2.3.1, 2.3.2 and 2.3.3) were used to measure apoptosis and these were compared to the microscope based comet assay (2.3.4). After 48hours of incubation, 1 ml of the isolated and irradiated cell suspension (4 x 10^5 cells) was aliquoted into 12 x 75 mm polystyrene flow cytometer tubes. The cell suspension was then centrifuged at 400 × g, the media was removed by invert and blot, and cells were held at 0°C until ready for analysis. All samples were analysed using a Beckman Coulter EPICS™ XL flow cytometer or by comet assay

2.3.1 Annexin V-FITC & 7-AAD

The Annexin V-FITC and 7-AAD assay was performed using a commercial kit (Beckman Coulter, Fullerton, CA). Briefly, a total of 4 x 10^5 cells were resuspended in 100 µl Binding Buffer. 10µl of Annexin V-FITC and 20 µl 7-AAD were added to the cell suspension. Samples were gently mixed and incubated at 0°C in the dark for 15min. After the incubation period, 400 µl binding buffer was added to all samples. Samples were analyzed by flow cytometry within 30 minutes. Lymphocytes were identified using forward and side scatter dot plots, a gate was drawn around the lymphocytes, and 10,000 events were collected in this gate. Annexin V-FITC and 7-AAD positive lymphocytes were measured by histogram plots based on gated events.

2.3.2 $DiOC_6$ & PI

A total of 4 x 10^5 cells were resuspended in 100µl of PBS. 1 µl 40nM $DiOC_6$ was added to each tube. Samples were mixed gently and incubated at room temperature in the dark for 15 minutes. Excess $DiOC_6$ was washed off by adding 2 ml of PBS to all tubes, centrifuged at 400 × g for 6 minutes and then, the supernatant was removed. The lymphocytes were resuspended in 100 µl PBS and 5 µl of 500 mg ml^{-1} PI solution was added. The samples were then mixed gently and incubated for 15 minutes in the dark at room temperature. Finally 400 µl PBS was added and then tubes were maintained at 0°C until analyzed by flow cytometry (within 30 minutes). Lymphocytes were identified by forward and side scatter dot plots, a gate was drawn around the lymphocytes, and 10,000 events were collected in this gate. $DiOC_6$ and PI positive lymphocytes were measured by dot plots based on gated events.

2.3.3 FITC Conjugated Active Caspase-3 Antibody Apoptosis Assay

The active caspase-3 assay was performed using a commercial apoptosis kit (BD PharMinagen, San Jose, CA). Briefly, 4 x 10^5 cells were resuspended in 500 µl Cytofix/Cytoperm™ Solution. Cells were incubated for 20 minutes on ice. Cells were then washed twice in 500 µl Perm/Wash™ Buffer (centrifuged at 400 × g, for 8 minutes). After the second wash cells were resuspended in 100 µl of Perm/Wash™ Buffer and 20 µl of FITC conjugated active caspase-3 antibody was added. Samples were incubated for 30 minutes at room temperature in the dark. After incubation cells were washed once in 1 ml Perm/Wash™ Buffer and resuspended in 500 µl

Perm/Wash™ Buffer. Samples were maintained at 0°C until analysis by flow cytometry. Lymphocytes were identified by forward and side scatter dot plots, a gate was drawn around the identified lymphocytes, a minimum of 10,000 events were collected. The amount of active FITC conjugated caspase-3 antibody positive were measured by a histogram plot based on gated events.

2.3.4 Comet Assay

Apoptotic lymphocytes were measured using a version of the neutral comet assay as previously described by McNamee *et al.*, 2000. A volume of culture containing 6,000 cells was made up to 27 µl and mixed with 243 µl of 1% low melting point agarose (Fisher Scientific, Middletown, VA) and pre-warmed to 42°C. A 90 µl sample of this mixture was cast into each of two individual wells of a two-well chamber (Nalge Nunc International, Rochester, NY) attached to Gelbond film (Mandel Scientific, Guelph, Ontario) as previously described (McNamee *et al*, 2000). The gels were left to dry at room temperature for 10 minutes. Once dry the gels were placed in lysis buffer (2.5 M NaCl, 100 mM tetrasodium EDTA (Tetrasodium Ethylenediamine Tetraacetate), 10mM Tris base [all from Fisher Scientific] and 1% N-lauryol sarcosine [Sigma Diagnostics, St. Louis, MO]. The lysis solution was supplemented with 1% Triton-X [VWR International, Mississauga, Ontario] prior to use. The gels were incubated in the lysis solution at 37°C for 1 hour. The gels were then rinsed with 18MΩ ultra pure milli-Q water and equilibrated for 30 minutes in 1x TAE buffer at room temperature. The gels were then placed in submarine agarose gel units (model HE-33, Hoeffer), containing 220ml 1 x TAE. The gels were then

electrophoresed for 2 minutes at 22 V (Power Pack model 401, Gibco-BRL). The gels were then rinsed three times in 18 MΩ water, followed by dehydration in 95% ethanol for a minimum of 2 hours and air dried overnight. The gels were stained with SBYR Gold nucleic acid stain (1:1,000 dilution of stock, Molecular Probes). Cells were analyzed using a fluorescent microscope (Zeiss Axiophat, Carl Zeiss MicroImaging, Inc Thornwood, NY) under a 200 × magnification with excitation wavelength of 520nm and emission of 580 nm. The percent apoptosis was calculated as (A/N) x 100, where A is the number of apoptotic cells over the total number of cells counted (N). Cells were classed as apoptotic based on their DNA fragmentation pattern as previously described (Kizilian *et al.*, 1999).

2.4 Kinetics of Gamma and Neutron Radiation-induced Apoptosis

Whole blood samples were exposed to 0 and 1 Gy of ^{137}Cs gamma and 280keV neutrons, at a dose rate of 2 Gy h^{-1}. Isolated lymphocyte samples were maintained in culture at 4.0 x 10^5 cells ml^{-1} for up to 96 hours. Samples were removed at intervals of 24 hours post-irradiation and assayed for the appearance of apoptotic cells using all four assays.

2.5 Dose Response

Whole blood samples were exposed to doses of 0, 0.25, 0.5, 1, 2 and 5 Gy of either gamma or 280keV neutron radiation. Samples were maintained in culture for 48 hours and then assayed using the three flow cytometry assays and the comet assay.

2.6 Gamma and 280kev Neutron Radiation Comparison

For the dose response curve, the effects of ^{137}Cs gamma and 280keV neutron irradiation were compared in blood samples from all three male individuals, of which one donor was repeated in triplicate. Samples were irradiated and assayed in parallel. Lymphocytes were then isolated, placed in supplemented medium at 4×10^5 cells ml^{-1} and incubated for 48 hours. After 48 hours samples were analyzed for apoptosis using the three flow cytometry assays and the comet assay.

2.7 Statistics

Mean values represent data from a minimum of five independent experiments (unless noted otherwise). Error bars were calculated as the standard error of the mean. *P*-values were calculated using the student's paired *t*-test.

3 RESULTS

3.1 Flow Cytometry

Results for flow cytometry experiments were gathered as described above (in section 2.3). $DiOC_6$ positive events were gated based on the unirradiated samples while PI positive gate was set according to a 2 Gy exposed sample (Figure 3-1). Annexin V-FITC positive and PI positive gates on the histogram plot were set based on the 2 Gy exposure sample (Figure 3-2). Similarly the caspase-3 positive gate on the histogram was set based on the 2 Gy exposures (Figure 3-3).

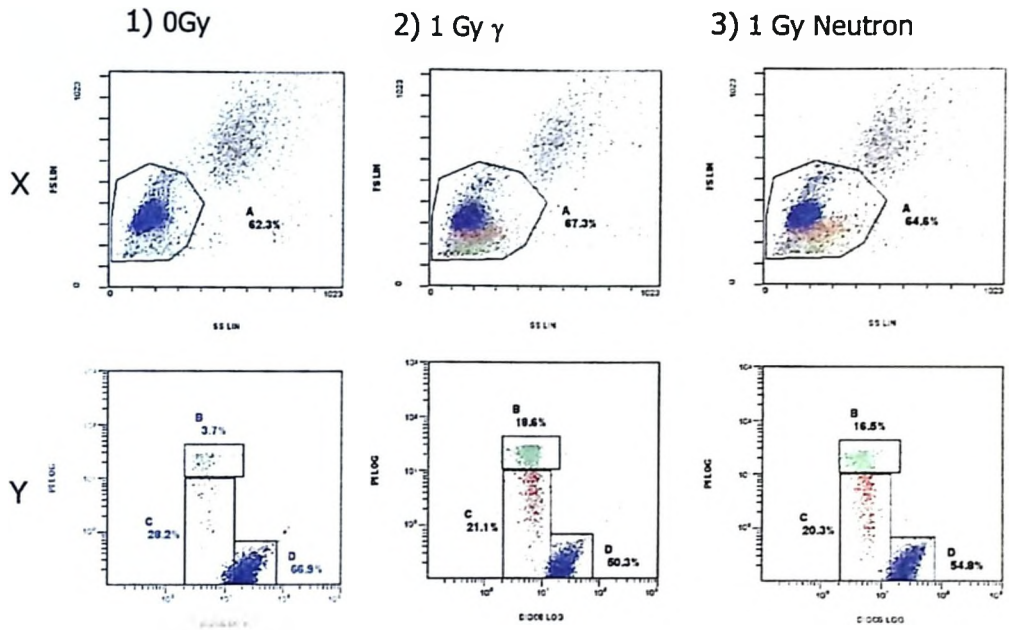

Figure 3-1. Lymphocytes identified based on forward and side scatter in the top row (X) of plots (Gate A). Amounts of $DiOC_6$ positive and PI positive lymphocytes were measured by dot plots (Y). $DiOC_6$ gate (D) was set using unirradiated samples, position of PI positive gate (B) was set using the sample exposed to 2 Gy and the dim $DiOC_6$ dim PI positive gate (C) was also set using the 2 Gy exposures. Dot plots were gated on lymphocytes. Column 1 shows response of unirradiated cells, cell exposed to 1 Gy ^{137}Cs gamma radiation are in column 2, and cells exposed to 1 Gy 280keV neutron are in column 3.

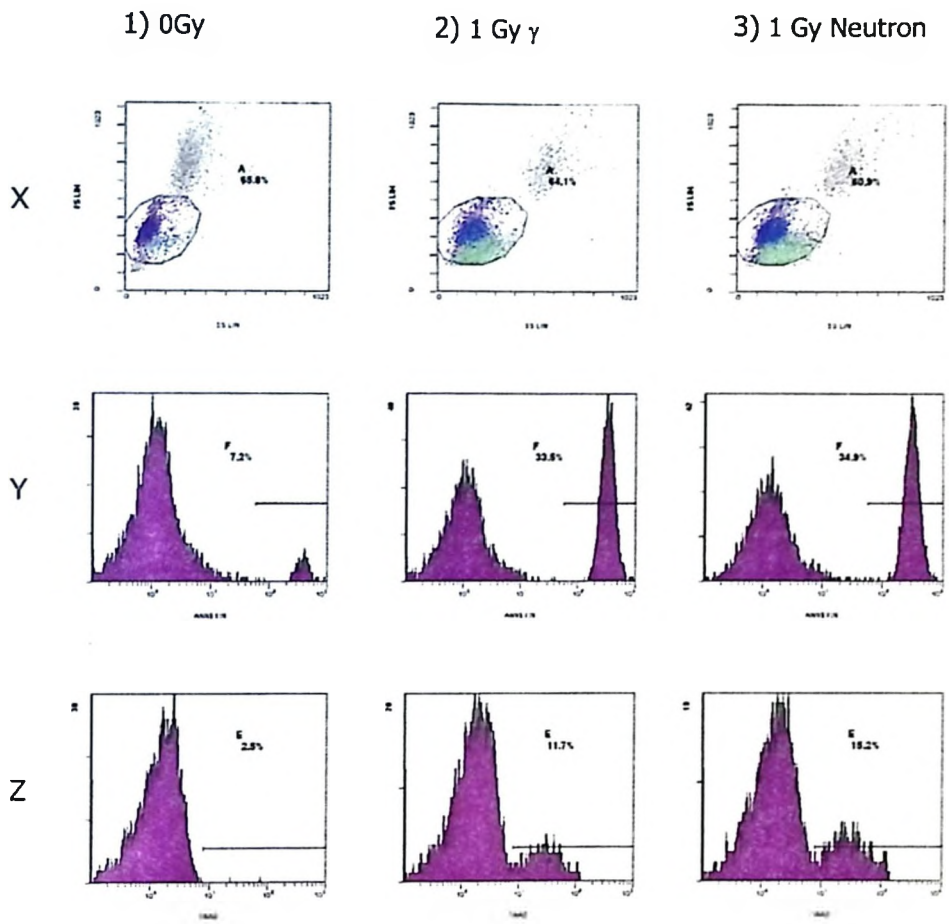

Figure 3-2. Lymphocytes identified based on forward and side scatter can be seen in the 1st row of plots (X). Amounts of Annexin V-FITC positive are measured by a histogram plot; with the percentage of the population staining positive marked by the bar gate (F) (middle row plots, Y). 7-AAD positive with the percentage of the population staining positive given by the bar gate (E) (bottom row plots, Z). Histogram plots were gated on lymphocytes. Column 1 shows response of unirradiated cells, cell exposed to 1 Gy ^{137}Cs gamma radiation are in column 2, and cells exposed to 1 Gy 280keV neutrons are in column 3.

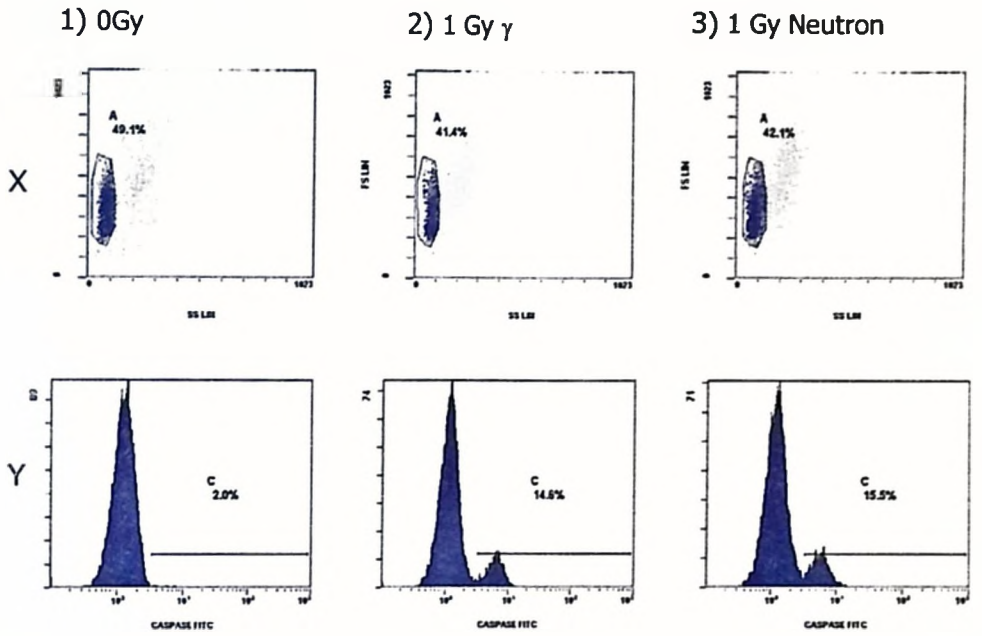

Figure 3-3. Lymphocytes identified based on forward and side scatter (X). Amounts of active caspase-3 FITC-conjugate positive lymphocytes were measured by a histogram plot gated on lymphocytes (Y); with the percentage of the population staining positive marked by the bar gate (C). The lymphocyte forward and side scatter pattern is altered due to the permeablization and fixation of cells during the staining procedure. Column 1 shows response of unirradiated cells, cell exposed to 1 Gy ^{137}Cs gamma radiation are in column 2, and cells exposed to 1 Gy 280keV neutrons are in column 3.

Table 3-1 Comparison of various flow apoptosis assays. The percentage of radiation-induced apoptosis by 1Gy of 280 keV neutrons or ^{137}Cs gamma (at 48 hours) as detected the six different markers is shown below. Measurements were corrected for spontaneous levels of apoptosis, the difference between apoptosis induced by neutron and gamma is shown. P-values were calculated using the students paired t-test.

	% Apoptosis			Significant Difference
Assay	1Gy Gamma	1Gy Neutron	Difference (neutron – Gamma)	p-value
$DiOC_6$	20.3 ± 10.2	22.9 ± 6.1	2.5	0.0590
PI	13.3 ± 2.3	12.5 ± 2.0	-0.8	0.2126
Annexin – V	25.2 ± 5.1	26.4 ± 5.2	1.2	0.4225
7-AAD	11.5 ± 5.2	14.0 ± 3.0	2.5	0.1646
Caspase	11.8 ± 2.6	9.5 ± 3.2	-2.0	0.2537
Comet	19.8 ± 3.6	20.2 ± 6.7	0.4	0.0830

The amount of radiation-induced apoptosis after exposure to 1 Gy 280keV neutrons or ^{137}Cs gamma radiation were compared Table 3-1). Table 3-1 illustrates that there was no significant difference ($p > 0.05$) between the amounts of apoptosis measured after exposure to 1 Gy of neutron or gamma radiation.

3.2 Kinetics of Radiation-Induced Apoptosis

Unirradiated lymphocyte samples assayed immediately after isolation had a spontaneous apoptotic frequency of 0.9% ± 0.4% by active caspase-3 analysis and 0.1% ± 0.1% by comet. Samples were incubated for up to 96 hours. Subsequent incubation in tissue culture caused a gradual increase in apoptosis of unirradiated control samples from 2.4% ± 0.5% at 24 hours to 2.5% ± 1.5% at 96 hours, as measured by Caspase-3 (Figure 3-4). The comet assay showed variation in apoptotic levels in control cultures from 5.6% ± 1.4% at 24 hours to 4.5% ± 2.33% at 72 hours. Levels of apoptosis in lymphocytes irradiated with 1 Gy ^{137}Cs or 280keV neutrons, increased with incubation. There was a significant difference between apoptotic levels of irradiated and unirradiated cells at 48 hours, this increasing trend continued with time and peaked at 72 hours post-irradiation for caspase-3 assay (Figure 3-4) but the comet assay peaked at 48 hours (Figure 3-5). Irradiated lymphocytes assayed using comet, 7-AAD and PI showed similar radiation-induced apoptosis kinetics.

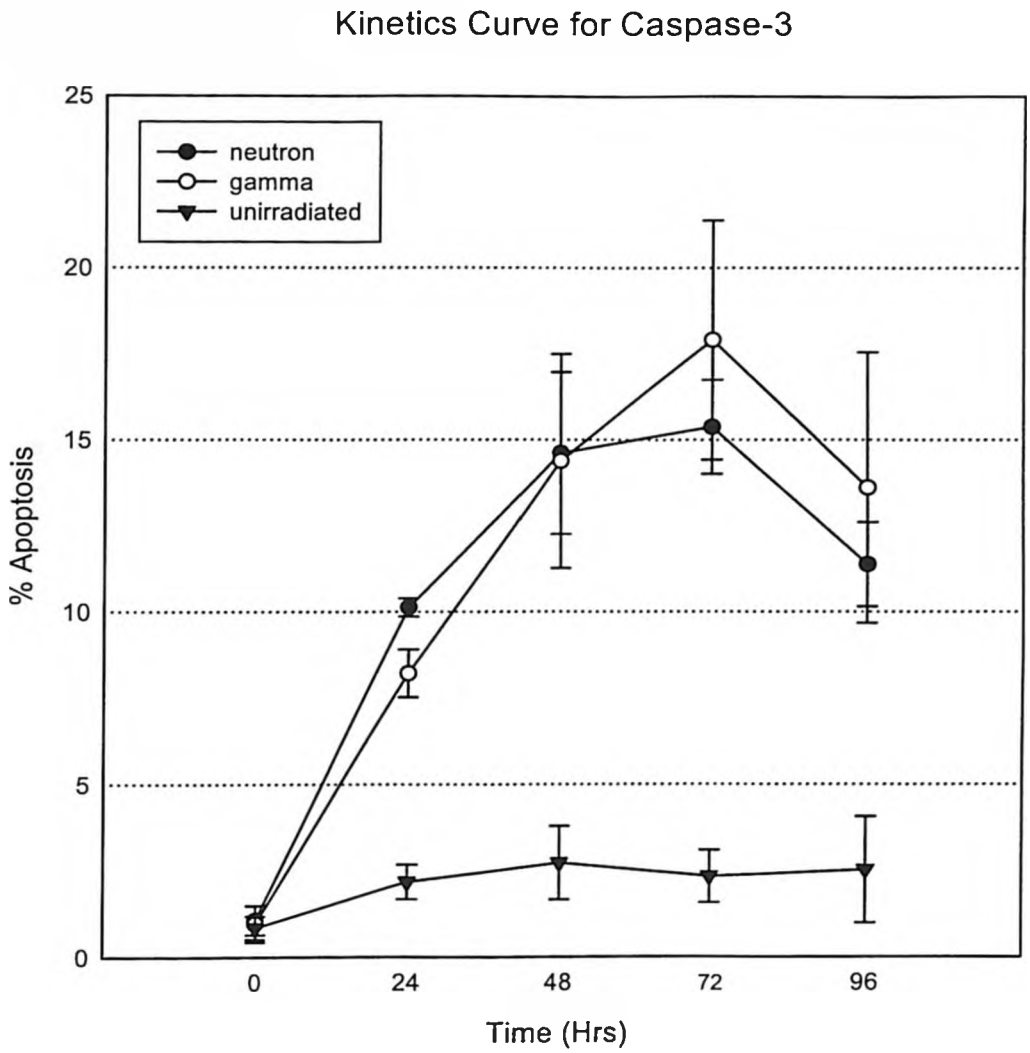

Figure 3-4. Kinetic curves for comparison of 280keV neutron (●) and ^{137}Cs gamma (○) radiation induction of apoptosis, in human lymphocytes after exposure to 1 Gy. Spontaneous induction of apoptosis in unirradiated lymphocytes is also shown (▼). Apoptosis was measured at different endpoints by the active caspase-3 assay. Data points are the mean of 3 independent experiments, errors are reported as the standard error of the mean.

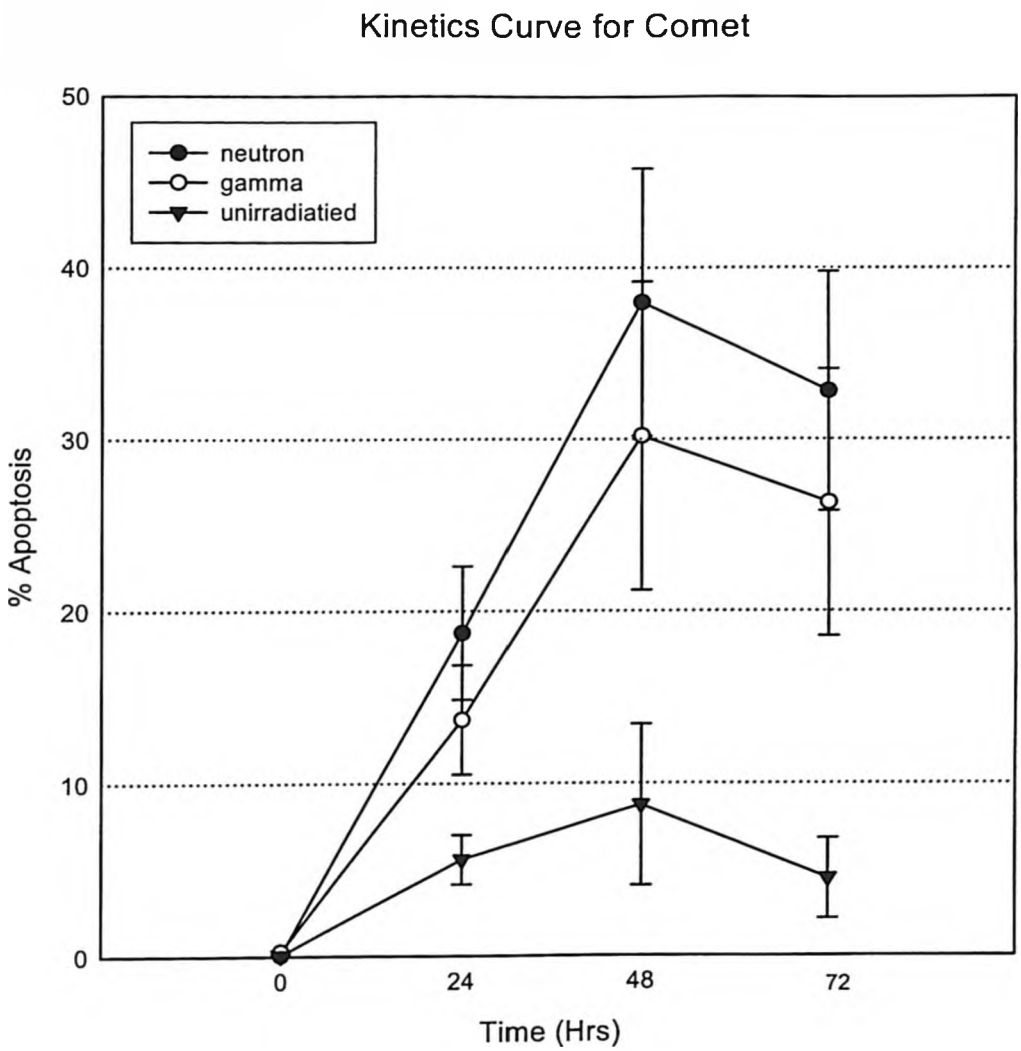

Figure 3-5. Kinetic curves for comparison of 280keV neutron (●) and ^{137}Cs gamma (o) radiation induction of apoptosis, in human lymphocytes after exposure to 1 Gy. Spontaneous induction of apoptosis in unirradiated lymphocytes is also shown (▼). Apoptosis was measured at different endpoints by the comet assay. Data points are the mean of 3 independent experiments, errors are reported as the standard error of the mean.

3.3 Dose Response

The mean value for radiation-induced apoptosis of five blood samples, from three different donors, of which one donor was repeated in triplicate are shown in Figure 3-6, Figure 3-7 and Figure 3-8. The $DiOC_6$, annexin -V, Caspase-3, 7-AAD, PI and comet assay results were all measured the induction of apoptosis at 48 hours which increased with increasing dose. The comet, annexin and $DiOC_6$ assays all had a higher level of background apoptosis when compared to the active caspase-3, PI and 7-AAD assays, which had a background apoptosis of less than 5%. A comparison of the dose response for the induction of apoptosis induced in lymphocyte samples at 48 hours, for 280keV neutron and ^{137}Cs radiation is shown, apoptosis levels measured for the comet assay (Figure 3-6 A), active caspase-3 assay (Figure 3-6 B), PI (Figure 3-7 A), $DiOC_6$ (Figure 3-7 B), Annexin –V (Figure 3-8 A) and 7-AAD (Figure 3-8 B). All assays showed an increasing dose response with both radiation qualities that was proportional to dose. No statistical difference between neutron and gamma induced apoptosis was observed ($p>0.05$) for any of the assays at doses except for a single point on the comet assay at 0.25 Gy (Figure 3-6 A, insert). The only data point to show a significant difference between gamma and neutron exposure was the manually scored comet assay, further study of the response of lymphocytes at low doses may be beneficial.

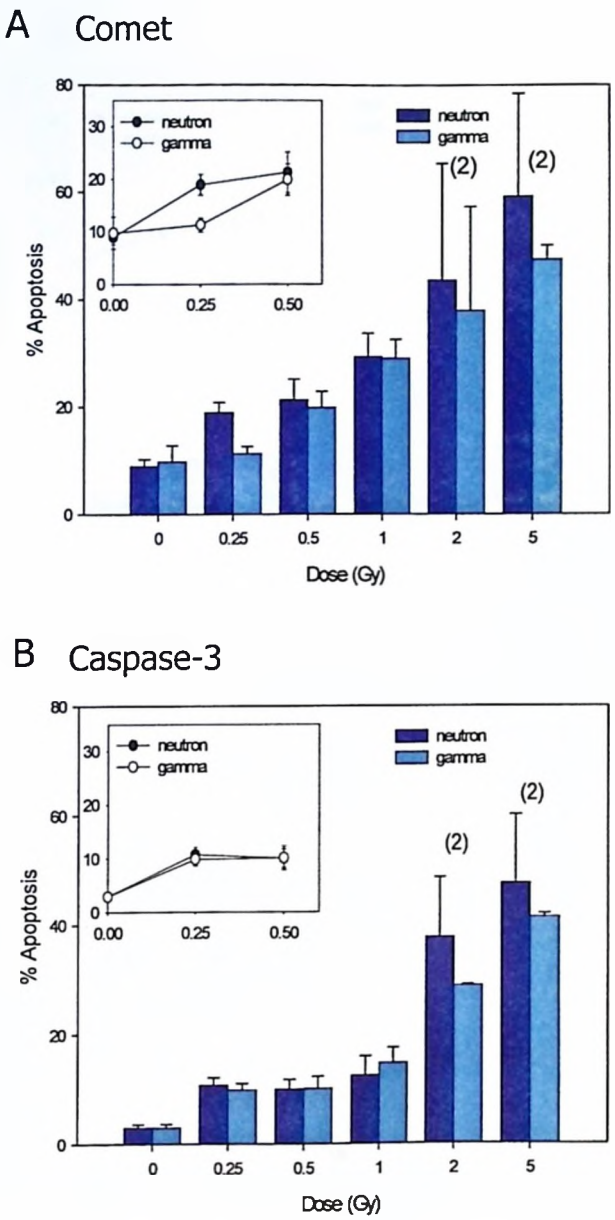

Figure 3-6. Dose response curves for comparison of 280keV neutron (▬) and ^{137}Cs gamma (▬) radiation induction of apoptosis, in human lymphocytes. Apoptosis was measured at different doses using the comet assay (A) and active caspase-assay (B). Data points are the mean of 5 independent experiments (unless otherwise noted); errors are reported as the standard error of the mean.

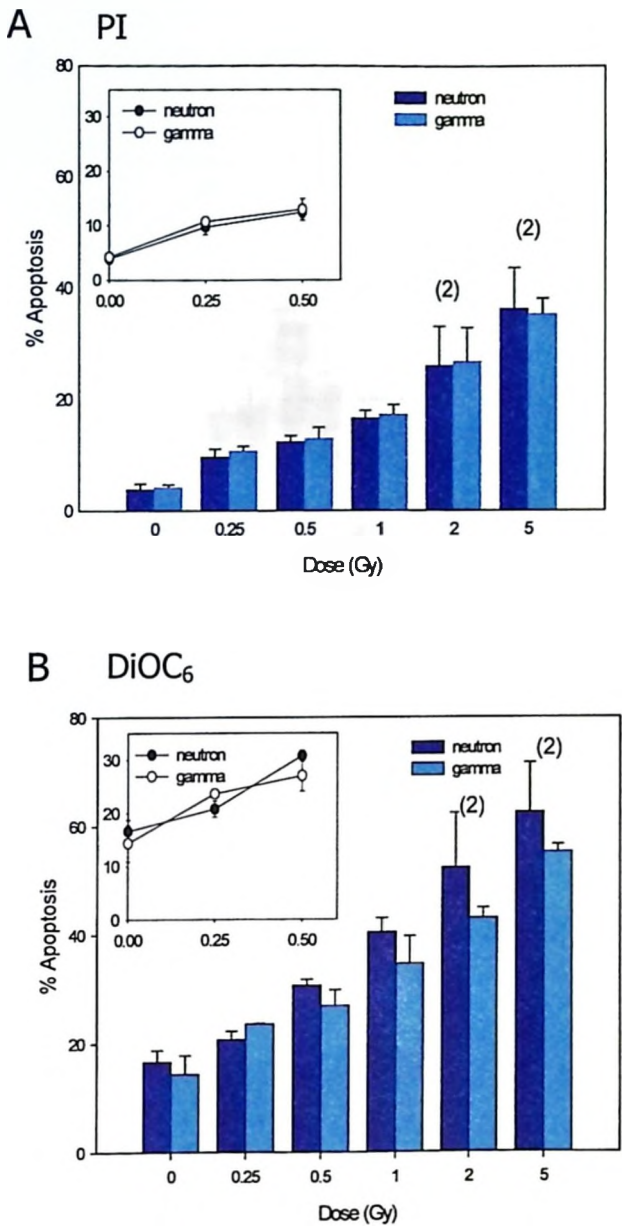

Figure 3-7. Dose response curves for comparison of 280keV neutron (▬) and ^{137}Cs gamma (▭) radiation induction of apoptosis, in human lymphocytes. Apoptosis was measured at different doses using $DiOC_6$ (A) and PI (B). Data points are the mean of 5 independent experiments (unless otherwise noted); errors are reported as the standard error of the mean.

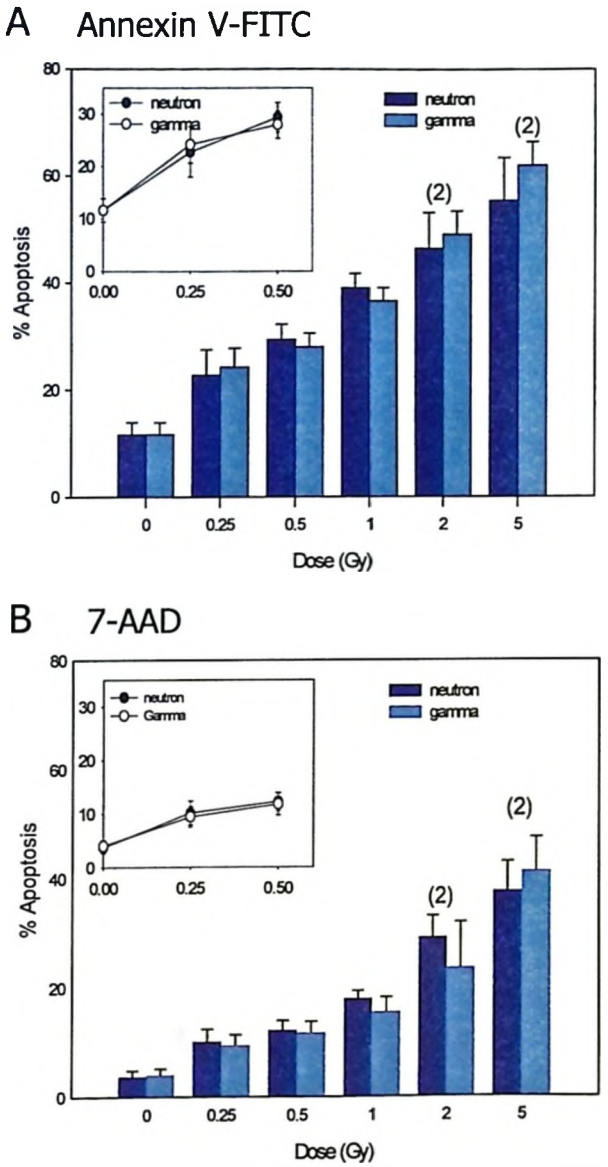

Figure 3-8. Dose response curves for comparison of 280keV neutron (▬) and ^{137}Cs gamma (▬) radiation induction of apoptosis, in human lymphocytes. Apoptosis was measured at different doses using the annexin V-FITC (A) and 7-AAD (B). Data points are the mean of 5 independent experiments (unless otherwise noted); errors are reported as the standard error of the mean.

Figure 3-9 shows the apoptotic response of human lymphocytes to gamma radiation at 48 hours as measured by annexin V-FITC and Caspase-3. The annexin V-FITC assay showed a rapid increase at lower doses (<1 Gy), but above 2 Gy annexin V-FITC has a saturated response and is less sensitive to changing doses. The caspase-3 assay is less sensitive than the Annexin V-FITC assay at low doses below 1Gy.

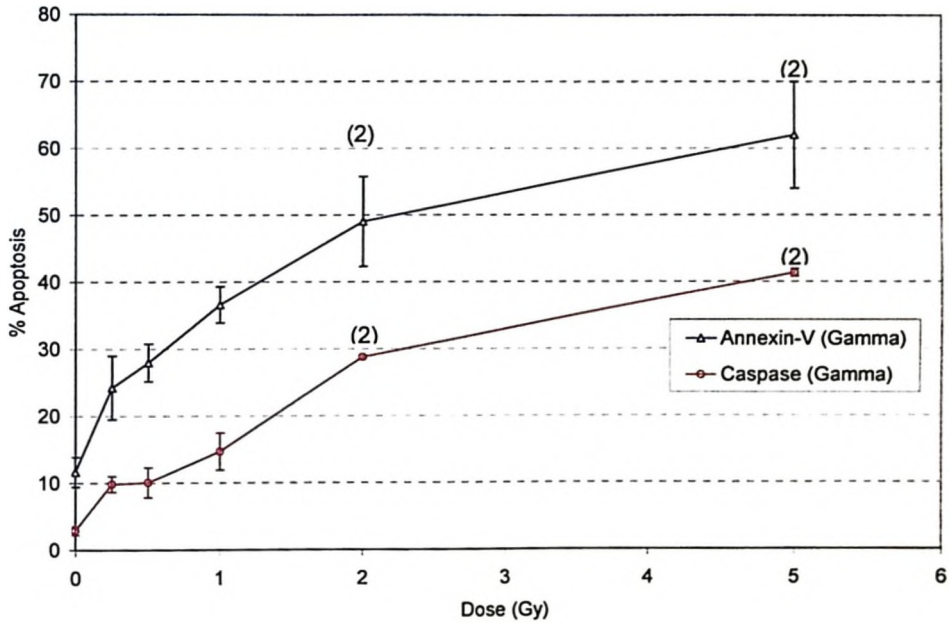

Figure 3-9. Dose response curves for ^{137}Cs gamma radiation-induced apoptosis, in human lymphocytes. Apoptosis was measured at 48 hours post-exposure by two cytometric assays Annexin V-FITC and Caspase-3. Apoptosis induced by ^{137}Cs gamma as measured by Annexin V-FITC (Δ) or Caspase-3 (o).Data points are the mean of 5 independent experiments (unless otherwise noted), errors are reported as the standard error of the mean

4 DISCUSSION

After exposure to ionizing radiation the majority of DNA damage is repaired 4 hours after the initial exposure. At longer incubation times, however DNA strand breaks begin to reappear (Cregan *et al*, 1999). This is believed to be due to the fragmentation of DNA as cells undergo apoptosis (Olive *et al*, 1993). It has previously been shown that human lymphocytes exposed to ionizing radiation undergo apoptosis *in vitro* at low doses with kinetics which might make this biological endpoint useful as a biological dosimeter (Ozsahin *et al*, 2003; Crompton *et al*, 1999; Menz *et al*, 1997; Boreham *et al*, 1996). It was also seen that lymphocytes exposed *in vitro* show a dose rate effect (Boreham *et al*, 2000). These experiments show similar dose responses and kinetics as those previously reported for low LET gamma radiation. Apoptosis was detected in human lymphocytes *in vitro* 24 hours post irradiation and levels continued to increase until a maximum was reached 48-72 hours later, depending on the assay being utilized.

It is generally accepted that high-LET radiation induces more DNA damage than low-LET radiation. Thus traditionally neutrons have been considered to have a high RBE. However, recently there have been conflicting results published describing the RBE of neutrons for cell killing (Table 1-1). Warenius and Down (1995) and Vral *et al.* (1998) have reported an RBE of unity for the induction of apoptosis in mouse thymocytes and human lymphocytes respectively. However reported RBE values between 3 and 4 have been reported for intestinal crypt cells (Hendry *et al.*, 1995), and RBE values of 1.3 to 3.0 for apoptosis in human lymphocytes (Meijer *et al* 1998) in

the case of fast neutrons. In the current study, we report that the amount of apoptosis induced in human lymphocytes was similar between gamma–ray and low energy neutron exposures. In this study, it was found that there was no statistical difference, for any given dose up to 5 Gy (after 48hrs of incubation) when samples were irradiated with either 280keV neutrons or ^{137}Cs gamma radiation. Which is in agreement with Warenius and Down (1995) and Vral *et al.* (1998) that neutrons have an RBE of one in the haematopoietic cells of mice.

4.1 Flow Cytometry

In this study, the kinetic curves showed that the expression of phosphatidylserine (annexin V-FITC), changes in mitochondrial membrane potential ($DiOC_6$) and plasma membrane degradation (PI and 7-AAD) reached a maximum at 48 hours. The caspase-3 expression peaked at 72 hours for both radiation qualities. Moreover the Caspase-3 assay was found to detect the lowest levels of spontaneous background levels of apoptosis, with a sizable increase in apoptotic levels with doses as low as 0.25Gy. Furthermore, the caspase-3 flow cytometer assay was also the simplest assay to analyze and interpret. A weakness of the caspase-3 assay was that it was relatively labour intensive, compared to other assays that needed less than 30 minutes. As caspase-3 is within the cell membrane, the lymphocytes must be fixed and permeablized during this assay. Therefore data on a single apoptotic parameter were gathered. Thus any variation of apoptotic levels in sub-populations of human lymphocytes as measured by caspase-3 as was not analyzed. The annexin V-FITC &

7-AAD assay is a rapid test, and yields information on the stage of cells during apoptosis, though this assay has a higher spontaneous background level of apoptosis. It may be possible to reduce this background level of apoptosis by looking at lymphocyte subpopulations using additional antibodies, such as CD3, CD4 and CD8 to detect B and T lymphocytes. As the annexin V-FITC & 7-AAD assay is performed on unfixed samples it provides the opportunity to conduct further studies on subpopulations of lymphocytes.

4.2 Relative Biological Effectiveness of 280keV Neutrons

In this study 280keV neutrons were found to induce apoptosis with the same effectiveness as ^{137}Cs gamma radiation. This result is not in agreement with previously published neutron RBE values for other neutron energies (Schmid *et al*, 2003, 2002, and 2000) (Table 1-1); when this work used was for the induction of chromosome aberrations as the biological endpoint. It has previously been reported that neutrons of energies between 36keV and 14.6MeV have an RBE ranging from 67.1 ± 28.9 to 16 ± 6.8 for induction of dicentrics in human lymphocytes, respectively (Schmid *et al*, 2003, 2002, and 2000). However, In order to measure chromosome aberrations in human lymphocytes a mitogen must be added to stimulate the resting cells to enter mitosis. However, when a mitogen is added to lymphocytes they are inhibited from committing apoptosis. This could mean that severely damaged cells, which otherwise would have died and be eliminated, are forced to divide and remain, resulting in a higher RBE. Thus the effect of neutrons to induce chromosome damage

under these experimental conditions is higher. Apoptosis is a radiation protection mechanism whereby cells are removed from the population routinely following damage.

The type of activation of the apoptosis signalling pathways could be another explanation for an RBE of unity for 280keV neutron radiation-induced apoptosis. DNA damage or death-receptor pathways could signal and initiate the cascade of events leading to apoptosis (Figure 1-2). It is possible that these signalling pathways triggered by cellular injury have a threshold. Consequently, if gamma and neutron radiation either cause damage to the DNA or activate CD95 receptor triggering the caspase cascade, the cell may commit apoptosis independent of radiation quality. The severity of DNA damage induced by the higher-LET source is above the minimum damage needed to activate the process and therefore irrelevant. It would be interesting to measure simultaneously the induction of apoptosis and chromosomal aberrations induced in the same human lymphocytes by the two radiation qualities. If an RBE value for the induction of chromosomal aberrations was found to be higher than that of radiation-induced apoptosis, this could further indicate that apoptosis has a threshold and is triggered as a protective response to eliminate cells exposed ionizing radiation. It is beneficial to an organism that a cell with damaged DNA commits apoptosis and is eliminated from the population rather than pass on a possible cancer causing mutation to daughter cells. In Figure 3-6 to Figure 3-8 it was seen that the RBE values are calculated based on radiation-induced apoptosis, for 280keV neutrons, in doses of less than 5 Gy were close to unity when compared to ^{137}Cs. These results are similar to those reported by Vral *et al* (1998) for apoptosis in resting human lymphocytes by 5.5 MeV fast neutrons. This is in agreement with a previous study

(Gajendiran *et al*, 2000), where it was shown that the RBE values calculated from comet assay results was generally lower than those calculated from chromosome aberration analysis.

4.3 Neutron Irradiation and Dosimetry Considerations

For this study, samples were irradiated with neutrons of a mean energy of 280keV created by a 3MV Van de Graff accelerator through a (p,n) reaction from a proton beam of 2.25MeV interacting with a thick lithium target. Samples were irradiated with a dose rate of 2.06 Gy h^{-1}; the highest dose rate which could be consistently achieved and reliably sustained by the accelerator when 2.25MeV proton energy was being used. A high dose rate was desired to minimize the time and consequently the amount of apoptosis occurring during irradiation, before lymphocytes were cultured. For this dose rate (2.06 Gy h^{-1}), a large current was generated at the target (45 – 55 μA); this current heated the thick lithium target which caused the target to melt frequently. On average targets were replaced after two experimental runs at the required proton energy and dose rate.

A further source of experimental variation which should be considered is the possibility of fractionation effects due to irradiation occurring at room temperature. In order to irradiate samples efficiently, a start and stop method was used. Two samples are placed in the neutron beam path and irradiated simultaneously. During a run the accelerator would be stopped and the first sample removed after the desired dose had been given and then the run would commence with the remaining sample until the

required dose had been achieved. The accelerator run would continue immediately, however, in the few minutes required to stop, remove sample and resume the accelerator, damaged lymphocytes would have started repairing thus possibly altering the effects of a single acute exposure.

The dose rate from the Van de Graff accelerator was monitored using an Anderson and Braun neutron rem counter (colloquially known as snoopy). The snoopy dosimeter was pre-calibrated, and placed at a distance of 2 m to prevent saturation and to allow for uniform irradiation (Kahn, 2003; Aslam, 2003d; Arnold, 2000). To relate to dose rate at 2 m to the dose rate of the samples the inverse square law was used. The snoopy, however, measures the equivalent dose in rem. The dose was converted to absorbed dose to tissue using a radiation quality factor calculated both experimentally and theoretically by Aslam (2003d) and used by others (Khan, 2003). The absorbed dose, D, was equal to the equivalent dose, H as measured by snoopy, divided by the radiation quality factor, Q. The use of a radiation quality factor of 13.2 to convert the equivalent dose to absorbed dose in Gray and then to argue that there is no RBE for 280keV neutrons appears to be a circular argument. However, the 13.2 radiation quality factor, Q, is a conversion factor, verified both experimentally and theoretically by Aslam *et al.* (2003b, c, d), and is a specific correction to the snoopy dosimeter for neutrons generated from a 2.25MeV proton beam.

An additional source of dosimetry uncertainty to be considered is the moderation of neutrons through the sample. Initially lymphocytes were isolated from whole blood prior to irradiation; the isolated lymphocytes were then irradiated in 50ml

polypropylene centrifuge tubes which have a 2.5cm diameter. In an attempt to minimise the moderation of neutrons, an isolated lymphocyte culture was kept in constant motion by gentle aeration. Unfortunately the gentle bubbling of sterile air through the sample caused the cells to disintegrate and only cellular debris was detected by the flow cytometer. Isolated lymphocytes in culture do not remain evenly distributed and fall out of suspension rapidly; therefore whole blood samples were irradiated in vacutainer tubes (1cm diameter). Irradiation in whole blood reduced the distance in which the neutrons could be moderated before interacting with cells, and kept cells more dispersed.

4.4 Future Directions

Since is has been possible to obtain a dose response curve for human lymphocytes after exposure to gamma and neutron radiation, it would be useful to see if it is possible to detect exposures *in vivo* to low doses of radiation. A group of people exposed to such doses would be patients undergoing diagnostic imaging techniques, for example those receiving a whole body CT-scan. For this work a blood sample would be obtained before and after the patient undergoes treatment. It may happen that the radiation-induced apoptosis is not adequate to measure directly and an additional *in vitro* dose would be required to induce measurable differences. These four groups of exposures would then be examined for radiation-induced apoptosis and chromosome aberrations. If apoptosis as a protective mechanism has been turned on to remove cells with damaged DNA from the organism, one should see an increase in

apoptosis. The first blood sample taken immediately before the patient undergoes whole body low dose irradiation and second sample is taken immediately following the procedure. These samples would be divided into two further sets, with one group being exposed to a further gamma dose *in vitro*. If an adaptive response is triggered the blood sample which got an *in vivo* priming dose would be expected to have fewer chromosome aberrations and may have an increased apoptotic response as apoptotic mechanisms become more efficient.

A study of chromosome aberration induced by radiation would be beneficial; to confirm that high-LET neutrons are inducing chromosomal aberrations with an RBE, which is in agreement with literature. It would be interesting to continue this work looking at how the RBE for human lymphocytes (for both the inducement of chromosome aberrations and apoptosis) is affected when the cells are exposed to different radiation qualities, such as alpha particles and varying neutron energies. This would require monoenergetic neutrons which could be accomplished using thin lithium targets.

5 CONCLUSION

Traditionally neutrons have been assigned a high RBE value. Data for these high RBE values were calculated based on increased levels of chromosomal aberrations induced by neutrons. However when radiation-induced apoptosis is used as the biological endpoint of interest it appears that there is no increased effectiveness in cell killing by 280keV neutrons compared to ^{137}Cs gamma radiation. Apoptosis is a radiation protection mechanism, which allows cells with genetically altered or damaged DNA to be eliminated from a tissue thus avoiding the risk of possible mutation and subsequent progression onto a cancer cell. This experiment may indicate that 280keV neutrons are no more damaging than gamma radiation, or that the surveillance system interprets gamma radiation-induced lesions in DNA as well as neutron typed lesions. It would seem that using apoptosis measured by flow cytometry for biological dosimetry has good potential in terms of sensitivity, reproducibility and efficiency. This biological endpoint could be very useful in the case of a large population that has been exposed due to accidental or deliberate acts. The fact that radiation quality may not affect the results further adds to the utility of this endpoint for biological dosimetry.

6 REFERENCES

Arnold, ML. Development of an accelerator based system for in-vivo neutron activation analysis measurements of manganese in humans, Ph. D. Thesis, McMaster University, Hamilton, ON, Canada. 2001.

Aslam, Prestwich WV, McNeill FE and Waker AJ. Investigating the TEPC radiation quality factor response for low energy accelerator based clinical applications. Radiat Prot Dosimetry. 103(4):311-22; 2003a.

Aslam, Prestwich WV, McNeill FE and Waker AJ. Development of a low-energy monoenergetic neutron source for applications in low-dose radiobiological and radiochemical research. Appl Radiat Isot. 58(6):629-42; 2003b.

Aslam, Prestwich WV, McNeill FE. Lithium target performance evaluation for low-energy accelerator-based in vivo measurements using gamma spectroscopy. Appl Radiat Isot. 58(3):321-31; 2003c.

Aslam, Spectrometry and Dosimetry for accelerator based in vivo measurements, PhD thesis. McMaster University, Hamilton, ON, Canada. 2003d.

Bauchinger M, Koester L, Schmid E, Dresp J, Streng S. Chromosome aberrations in human lymphocytes induced by fission neutrons. Int J Radiat Biol Relat Stud Phys Chem Med. 45(5): 449-57; 1984.

Belka C, Heinrich V, Marini P, Faltin H, Schulze-Osthoff K, Damberg and Budach. Ionizing radiation and the activation of caspsae-8 in highly apoptosis-sensitive lymphoma cells. Int. J. Radiat. Biol. 75(10): 1257-1264; 1999.

Boreham DR, Dolling J-A, Maves SR, Siwarungsun N and Mitchel REJ. Dose-rate effects for apoptosis and micronucleus formation in gamma-irradiated human lymphocytes. Radiat. Res. 153: 579-586; 2000.

Boreham DR, Gale KL, Maves SR, Walker JA and Morrison DP. Radiation-induced apoptosis in human lymphocytes: potential as a biological dosimeter. Health Phys. 71(5): 685-691; 1996.

Britten RA, Peters LJ and Murray D. Biological factors influencing the RBE of neutrons: Implications for the past, present and future use in radiotherapy. Radiat. Res. 156: 125-135; 2001.

Budihardjo I, Oliver H, Lutter M, Luo X and Wang X. Biochemical pathways of caspase activation during apoptosis. Annu Rev Cell Dev Biol. 15: 269-290; 1999.

Castedo M, Hirsch T, Susin SA, Zamzami N, Marchetti P, Macho A, and Kroemer G. Sequential acquisition of mitochondrial and plasma membrane alterations during early lymphocyte apoptosis. J. Immunol. 157: 512 – 521; 1996.

Cregan SP, Boreham DR, Walker PR, Brown DL and Mitchel RE. Modification of radiation-induced apoptosis in radiation- or hyperthermia-adapted human lymphocytes. Biochem Cell Biol. 72(11-12): 475-82; 1994.

Cregan SP, Smith BP, Brown DL and Mitchel REJ. Two pathways for the induction of apoptosis in human lymphocytes. Int. J. Radiat. Biol. 75(9): 1069-1086; 1999.

Crompton NE, Miralbell R, Rutz HP, Ersoy F, Sanal O, Wellmann D, Bieri S, Coucke PA, Emery GC, Shi YQ, Blattmann H, Ozsahin M. Altered apoptotic profiles in irradiated patients with increased toxicity. Int J Radiat Oncol Biol Phys. 45(3):707-14; 1999.

Cryns V and Yuan J. Proteases to die for. Genes Dev. 12:1551–1570: 1998.

Edwards AA, Neutron RBE values and their relationship to judgments in radiological protection. J. Radiol. Prot. 19(2): 93-105; 1999.

Fabry L Leonard A, amd Wambersie A. Induction of chromosome aberrations in G0 human lymphocytes by low doses of ionizing radiation of different quality. Radiat. Res. 103: 122-134; 1985.

Fadok VA, Voelker DR, Campell PA, Cohen JJ, Bratton DL and Henson PM. Exposure of Phosphatidylserine on the surface of apoptotic lymphocytes triggers specific recognition and removal by macrophages. The Journal of Immunology. 148(7): 2207-2216; 1992.

Gajendiran N, Tanaka and Kamada N. Comet assay to sense neutron 'fingerprint'. Mutat. Res. 452: 179-187: 2000.

Goodhead DT. Initial events in the cellular effects on ionizing radiations: Clustered damage in DNA. Int. J. Radiat. Biol. 65(1): 7-17; 1994.

Gorczyca W, Gong J and Darzynkiewicz Z. Detection of DNA strand breaks in individual apoptotic cells by the in situ terminal deoxynucleotydyl transferase and nick translation assays. Cancer Res. 23; 1945-1951; 1993.

Gown AM and Willlingham MC. Improved detection of apoptotic cells in archival paraffin sections: Immunohistochemistry using antibodies to cleaved caspase-3. The Journal of Histochemistry and Cytochemistry. 504(4); 449-454; 2002.

Hendry JH, Potten CS and Merritt A. Apoptosis induced by high and low-LET radiations. Radiat Env. Biophys. 34: 59-62; 1995.

Hertveldt K, Philippe J, Thierens H, Cornelissen M, Vral A, amd De Ridder L. Flow cytometry as a quantitative and sensitive method to evaluate low dose radiation-induced apoptosis I*in vitro* in human peripheral blood lymphocytes. Int. J. Radiat. Biol. 71(4): 429-433; 1997.

Kerr JFR, Wyllie AH and Currie AR. Apoptosis a basic biological phenomenon with wide-raging implications in tissue kinetics. Br J Cancer. 26: 239-257; 2000..

Khan RFH, Electron paramagnetic resonance biophysical radiation dosimetry with tooth enamel, Ph. D. Thesis, McMaster University, Hamilton, ON, Canada. 2003.

KizilianN, Wilkins RC, Reinhardt P, Ferarotto C, McLean JRN and McNamee JP. Silverstained comet assay for detection of apoptosis. Biotechniques. 27: 926-929; 1999.

Kroemer G and Reed JC. Mitochondrial control of cell death. Nat Med. 6(5); 513-519; 2000.

Kroemer G. Mitochondrial control of apoptosis: an introduction. Biochem Biophys Res Commun. 304(3):433-5; 2003.

Loo D and Rillema J. Measurements of cell death. Methods Cell Biol. 57: 251-264; 1998.

Martinou JC. Key to the mitochondrial gate. Nature. 399: 411-412; 1999.

McNamee JP, McLean JR, Ferrarotto CL, Bellier PV. Comet assay: rapid processing of multiple samples. Mutat Res. 466(1):63-9; 2000.

Meijer AE, Kronqvist ISE, Lewensohn R and Harms-Ringdahl M. RBE for the induction of apoptosis in human peripheral lymphocytes exposed *in vitro* to high-LET radiation gererated by accelerated nitrogen ions. Int J. Radiat. Biol. 73(2): 169-177; 1998.

Menz R, Andres R, Larsson B, Ozsahin M, Trott K, Crompton NE. Biological dosimetry: the potential use of radiation-induced apoptosis in human T-lymphocytes. Radiat Environ Biophys. 36(3):175-81; 1997.

Olive PL, Frazer G and Banath JP. Radiation induced apoptosis measured in TK6 human B lymphoblast cells using the comet assay. Radiat. Res. 136: 130-136; 1993.

Overbeeke R, Steffens-Nakken H, Vermes I, Reutelingsperger C, and Haanen C. Early features of apoptosis detected by four different flow cytometry assays. Apoptosis. 3(2):115-21; 1998.

Ozsahin M, Li L, Crompton NE, Shi Y, Zouhair A, Coucke PA, Mirimanoff RO, Azria D. Radiation-induced late toxicity can be predicted by CD4 and CD8 T-lymphocyte apoptosis: results of a prospective study in 399 individual consenting patients. Int J Radiat Oncol Biol Phys. 57(2 Suppl):S203-4; 2003.

Prasanna PG, Kolanko CJ, Gerstenberg HM, Blakely WF. Premature chromosome condensation assay for biodosimetry: studies with fission-neutrons. Health Phys. 72(4): 594-600; 1997.

Rasola A and Geuna M. A flow cytometry assay simultaneously detects independent apoptotic parameters. Cytometry 45: 151-157; 2001.

Saini KS and Walker NI, Biochemical and molecular mechanisms regulating apoptosis. Molecular and Cellular Biochemsitry 178: 9-25: 1998.

Schmid E, Regulla D, Guldbakke S, Schlegel D and Roos M. Relative Biological Effectiveness of 144keV Neutrons in Producing Dicentric Chromosomes in Human Lymphocytes Compared with ^{60}Co Gamma Rays under Head-to-Head Conditions. Radiat. Res., 157: 453-460; 2002.

Schmid E, Regulla D, Schlegel D and Bauchiner M. The Effectiveness of Monoenergetic Neutrons at 565kV in Producing Dicentric Chromosomes in Human Lymphocytes at Low Doses. Radiat. Res., 154: 307-312; 2000.

Schmid E, Schlegel D, Guldbakke S, Kapsch R-P and Regulla D. RBE of nearly monoenergetic neutrons at energies of 36keV-14.6Mev for induction of dicentrics in human lymphocytes. Radiat. Environ. Biophys., 42: 87-94; 2003.

Schultz DR and Harrington WJ. Apoptosis: Programmed Cell Death at a Molecular Level. Seminars in Arthritis and Rheumatism. 32(6): 345-369; 2003.

Sgnoc R and Gruber J. Apoptosis Detection: An Overview. Experimental Gerontology. 33(6): 525-533; 1998.

Sgonc R, Boeck G, Dietrich H, Gruber J, Recheis H and Wick G. Simultaneous determination of cell surface antigens and apoptosis. Trends in Genetics. 10: 41-42; 1994.

Shapiro, HM. Practical Flow Cytometry, 4th edition. John Wiley and sons, Inc. Chapters 1, 4 and 7; 2003.

Steller H. Mechanisms and genes of cellular suicide. Science 267: 1445-1449; 1995.

Strasser A, O'Conner L and Dixit VM. Apoptosis signalling. Annu Rev Biochem 69: 217-245; 2000.

Van Engeland M, Nieland LJW, Ramaekers FCS, Schutte B and Reutelingsperger CPM. Annexin V Affinity Assay: A review on a apoptosis detection system based on phosphatidylserine exposure. Cytometry. 31: 1-9; 1998.

Vermes I, Haanen C and Reutelingsperger C. Flow Cytometry of Apoptotic Cell Death. J. Immunol Methods. 243: 167-190; 2000.

Vermes I, Hannen C, Steffens-Nakken H and Reutelingsperger C. A novel assay for apoptosis. Flow cytometry detection of phosphatidylserine expression on early apoptotic cells using fluorescein labelled Annexin V. J. Immunol Methods. 184: 39-51; 1995.

Vral A, Cornelissen M, Thierens H, Louagie h, Philippe J, Strijckmans K and De Ridder L. Apoptosis induced by fast neutrons versus ^{60}Co γ-rays in human peripheral blood lymphocytes. Int. J. Radiat. Biol. 73(3): 289-295; 1998.

Warenius HM and Down JD. RBE of fast neutrons for apoptosis in mouse thymocytes. Int. J. Radiat. Biol. 68: 625-629: 1995.

Wyllie AH. Apoptosis and the regulation of cell number in normal and neoplasmic tissues: an overview. Cancer Metastasis Rev 11: 95-103; 1995.

Wilkins RC, Kutzner BC, Troung M, Sanchez-Dardon J and McLean JRN. Analysis of radiation-induced apoptosis in human lymphocytes: Flow cytometry using annexin V and Propidium Iodide versus the neutral comet assay. Cytometry 48: 14-19; 2002.

Willingham MC, Cytochemical Methods for the Detection of Apoptosis. J Histochem Cytochem. 47(9): 1101-1109; 1999.

7 APPENDIX A

Quantification of Peptides Binding Affinity for Radiopharmaceutical Development.

A.1 Introduction

A collaborative project was developed between Drs. D. Boreham and J. Valliant. This project offered me the opportunity to acquire the required expertise and technological skills for operating a flow cytometer which enabled me complete the work in this thesis. This work has been presented at the Society of Nuclear Medicine's 51st annual meeting* and published by the Journal of Bioconjugate Chemistry†

An important part of radiopharmaceutical development is the ability to quantify the binding affinity of novel peptides to their target cells. Cellular Receptor-

---

*. K. A. Stephenson, J. F. Valliant, J. Zubieta, S. R. Banerjee, M. K. Levadala, D. R. Boreham, K. Maresca, J. W. Babich A Versatile Automated Solid-Phase Synthesis Strategy For The Preparation Of Re(I)/Tc(I).

† Stephenson KA, Zubieta J, Banerjee SR, Levadala MK, Taggart L, Ryan L, McFarlane N, Boreham DR, Maresca KP, Babich JW, Valliant JF. A new strategy for the preparation of peptide-targeted radiopharmaceuticals based on an fmoc-lysine-derived single amino acid chelate (SAAC). Automated solid-phase synthesis, NMR characterization, and in vitro screening of fMLF(SAAC)G and fMLF[(SAAC-Re(CO)3)+]G.
Bioconjug Chem. 2004 Jan-Feb; 15(1):128-36.

Ligand binding can be observed by flow cytometry. Flow cytometry offers the advantage of being able to monitor ligand binding to individual cells in real time and gives measurements in relative fluorescence intensity scale. In order to get quantitative information on binding affinities of novel peptides it is necessary to convert relative fluorescence readings to the number of bound ligands using an appropriate calibration method (Hoffman *et al,* 1996; Waller *et al,* 2001).

Throughout this study the binding affinity of two novel peptides to lymphocytes was investigated in collaboration with the Department of Chemistry, McMaster University. Leukocyte samples were run on a Beckman Coulter EPICS® XL flow cytometer. To convert the amount of relative fluorescence measured to the number of bound ligands, the flow cytometer was calibrated with fluorescein isothiocyanate (FITC) labelled beads (Quantum 26 Beads, Bangs Laboratories, Inc, Fischer, IN.) prior to sample analysis. The fluorescence intensity of the beads was provided by the manufacture in units of Molecules of Equivalent Soluble Fluorochrome (MESF) and ranged from 5300 to 468,800. A linear fit of MESF versus the mean channel number of the beads was then plotted to convert the mean channel number of all subsequent samples to MESF values (Figure A-7-1).

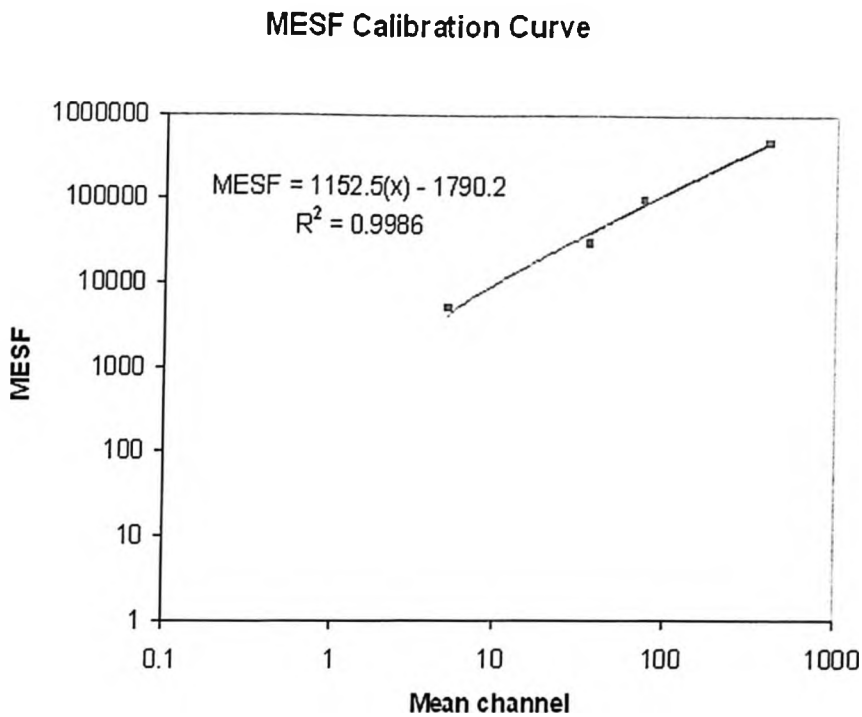

Figure A-7-1. A plot of mean channel number versus molecules of equivalent soluble fluorescence (MESF) is drawn. Using the calibration curve equation it is possible to quantify the level of fluorescence for the peptides in terms of MESF

Direct measurement of the binding affinity is not possible, as the novel peptides being investigated were not fluorescent. Fluorescent tags were not added, since the addition of a tag may alter the binding properties. To overcome this difficulty competitive binding, an indirect measuring technique, was utilized. Knowing binding information of the fluorescent ligand in solution along with a known

concentration of cells, it is possible to calculate indirectly the binding of the unlabelled ligand based on its affect on the binding of the fluorescent ligand.

A.2 Materials and Methods

A.2.1 Neutrophil Preparation

Whole human blood (10-15 mL) was collected in vacutainer tubes (Becton Dickinson) containing sodium heparin. The red blood cells were lysed using a modified ammonium chloride method. One part whole blood was diluted and mixed immediately with 23 parts of pre-warmed ammonium chloride solution. The 0.145 M ammonium chloride solution contained 1.5 mM potassium bicarbonate and 0.1 mM EDTA). Tubes containing the ammonium chloride solution and whole blood were incubated at room temperature for 15 min and then centrifuged in a Beckman Coulter Allegra 6R centrifuge at 400 × g for 7 min at 5°C. The supernatant was removed and the pellet of leukocytes subsequently resuspended in Hanks Balanced salt solution (HBSS) containing 0.1% BSA, 10 mM HEPES, and 1.5 mM $CaCl_2$, henceforth known as HBSS+. The cells were spun for 7 min at 400 × g at 5°C, the supernatant removed, and the pellet was resuspended in HBSS+. Cell counts were performed using a haemocytometer and a Beckman Coulter Z2 Coulter Particle Counter and Size Analyzer. Cell concentrations were then adjusted to 2×10^6 mL^{-1}.

A.2.2 Equilibrium Binding Assay

The equilibrium binding assay was used to determine the number of formyl peptide receptors (FPRs) on the surface of the neutrophils and the dissociation constant (K_d) of the fluorescein-labelled fNLFNTK (Molecular Probes) (1.0 nM) by preparing a saturated binding curve of the fNLFNTK concentrations versus fluorescence intensity.

Stock solutions of the novel peptide were made by dissolving the peptide derivatives in DMSO and then diluting with HBSS+ to the desired concentrations, while ensuring that the concentration of DMSO was less than 0.1%. Cells at a concentration of 1×10^{6} ml^{-1} were equilibrated with 0.25, 0.5, 1.0, 3.0, 5.0, 10.0 and 20.0 nM solutions of the novel peptide derivative in duplicate. The samples were incubated for 2 hours at 0°C in the dark and then run on the flow cytometer. The neutrophil population was identified on the basis of forward and side scatter parameters using Expo 32 ADC software (Beckman Coulter). All samples were repeated in the presence of 30 μM fMLF to account for non-specific binding. Figure A-7-2 shows the number of receptor-ligand complexes per cell (B). This was determined using the following equation, where Q is a normalisation factor used by Waller *et al.* (2001) and F is the total fluorescence per cell:

$$B\,(\text{in ligand bound per cell}) = F\left(\frac{MESF}{Cell}\right) \times Q$$

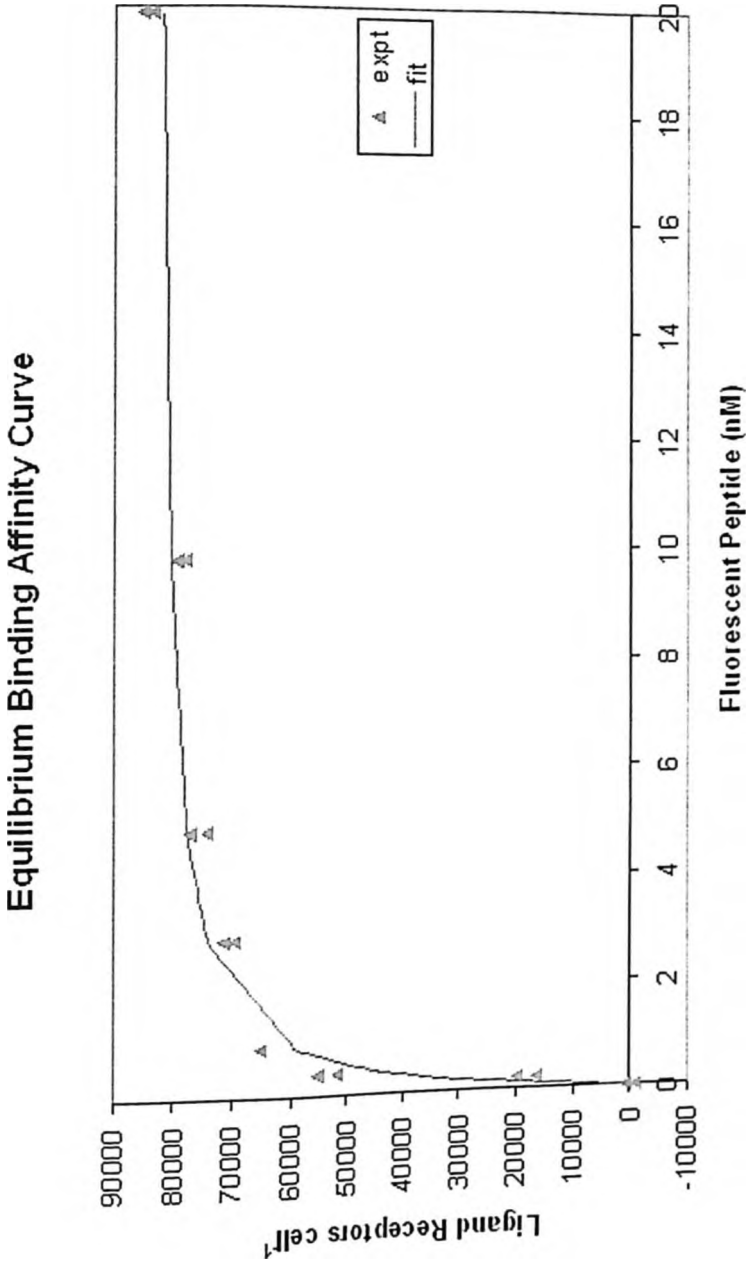

Figure A-7-2. Equilibrium binding curve. Representative equilibrium binding curve of receptor-ligand complexes normalized to the experimental R_{tot} versus ligand concentration.

The level of non-specific binding did not vary significantly with concentration of labelled peptide. Thus an average value of non-specific binding was subtracted from the fluorescence per cell, F, when determining the number of receptor – ligand complexes. The total number of N-formyl peptide receptors, R_{tot}, and the equilibrium dissociation constant, K_d, were evaluated by minimising the squared residual of the equilibrium solution using a one-site binding model, as described on the equation below. Figure A-7-3 shows the line of best fit for the experimental data collected form the flow cytometer which was used to calculate R_{tot}, and K_d. The values of R_{tot}, and K_d for each donor were solved simultaneously.

$$[LR] = \frac{R_{tot}[L]}{[L] + K_d}$$

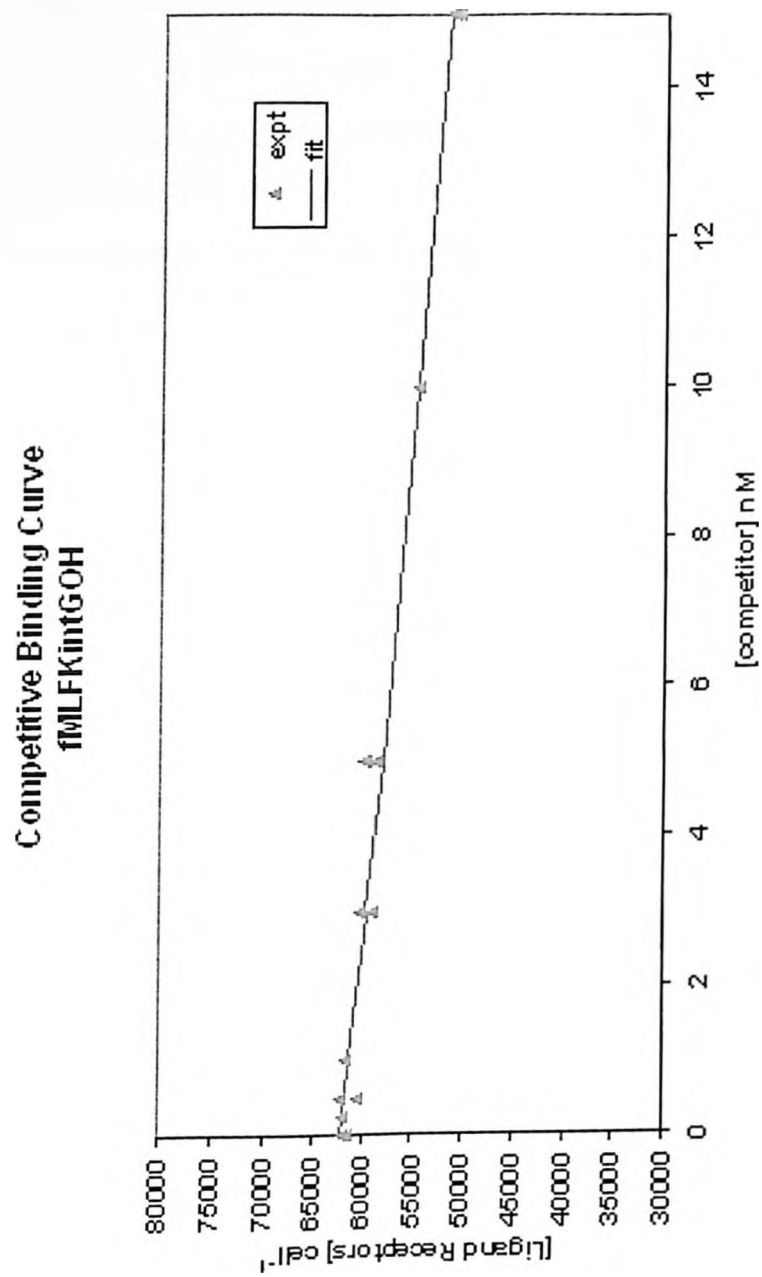

Figure A-7-3. Competitive binding curve for unlabelled ligands.

Results and Discussion

Table A-7-1. Dissociation Constants for the reference peptide fMLF and the novel peptides of interest.

Peptide	K_d (nM)
fMLF	32 ± 2.8
fMLF(SAAC)G	19 ± 3.4
fMLF[(SAAC – $Re(CO)_3)^+$]G	9 ± 0.8

The dissociation constants for the competing unlabeled ligands (K_d) for a reference peptide and novel peptides are shown in Table A-7-1. The K_d for each ligand was determined by fitting the specific ligand using the one-site binding model as described by Waller *et al.* (2001). The reference peptide chosen was fMLF; the K_d value reported in Table A-7-1 is in good agreement with the published values (Fay *et al.*, 1991)

Traditionally radioligand biological properties are measured by animal studies, which are costly, labour intensive and time consuming. These methods are not practical when evaluating a library of compounds. In this work a flow cytometric method was established to assess ligand – receptor interactions. Flow cytometry has several advantages over traditional methods; flow cytometry allows real time studies on single cells. Flow cytometry also allows the study of ligand binding to specific

subpopulations, in this study it was seen that the compounds fMLF(SAAC)G and fMLF[(SAAC – $Re(CO)_3)^+$]G preferentially bind to neutrophils, rather than just granulocytes as a whole. This screening project showed that the novel compounds fMLF(SAAC)G and fMLF[(SAAC – $Re(CO)_3)^+$]G bind to the granulocytes with affinities greater than the parent fMLF peptide, which was used as the reference peptide. This study indicated that fMLF(SAAC)G is a promising agent for targeting ^{99m}Tc to FPR receptors.

A.4 Conclusion

Flow cytometry can be used as a powerful screening tool, which affords the opportunity to identify rapidly compounds that are capable of selectively targeting specific types of granulocytes.

A.5 References

Fay SP, Posner RG, Swann WN and Sklar LA. Real-time analysis of the assembly of ligand, receptor, and G protein by quantitative fluorescence flow cytometry. Biochemistry. 30(20):5066-75; 1991.

Hoffman JF, Keil ML, Riccobene TA, Omann GM and Linderman JJ. Interconverting receptor states at 4°C for the neutrophil N-formyl peptide receptor. Biochemistry. 35(40):13047-55; 1996.

Waller A, Pipkorn D, Sutton J, Linderman J and Omann G. Validation of flow cytometric competitive binding protpcols and characterization of fluorescently labelled ligands. Cytometry. 45: 102-114; 2001.